

HAMED ALINEZHAD KORDI

**METAL TRANSFER MAPPING FOR FCAW PROCESS
BY USING NEAR-INFRARED FILMING**



FEDERAL UNIVERSITY OF UBERLANDIA
FACULTY OF MECHANICAL ENGINEERING

2016

HAMED ALINEZHAD KORDI

**METAL TRANSFER MAPPING FOR FCAW PROCESS BY USING
NEAR-INFRARED FILMING**

Dissertation presented to the Postgraduate Program of Mechanical Engineering at Federal University of Uberlandia, as a part of requirements for obtaining the title of **MASTER IN MECHANICAL ENGINEERING.**

Concentration Area: Materials and Manufacturing Processes.

Supervisor: Prof. Dr. Louriel O. Vilarinho

**UBERLANDIA - MG
2016**

Dados Internacionais de Catalogação na Publicação (CIP)
Sistema de Bibliotecas da UFU, MG, Brasil.

A411m Alinezhad Kordi, Hamed, 1989-
2016 Metal transfer mapping for FCAW process by using near-infrared
 filming / Hamed Alinezhad Kordi. - 2016.
 87 f. : il.

 Orientador: Louriel Oliveira Vilarinho.
 Dissertação (mestrado) - Universidade Federal de Uberlândia,
Programa de Pós-Graduação em Engenharia Mecânica.
 Inclui bibliografia.

 1. Engenharia mecânica - Teses. 2. Soldagem elétrica - Teses. I.
Vilarinho, Louriel Oliveira, 1975-. II. Universidade Federal de
Uberlândia. Programa de Pós-Graduação em Engenharia Mecânica. III.
Título.

CDU: 620

I dedicate my dissertation to my parents. A special feeling of gratitude to my lovely parents “Mehran and Manizheh”.

My siblings, nephews and nieces have never left my side and are very special. Also dedicate this dissertation to my many friends who have supported me throughout the process.

ACKNOWLEDGEMENTS

There have been many people who have walked alongside me during the last two years. They guided me, placed opportunities in front of me and showed me the doors that might be useful to open.

Firstly, I would like to express my sincere gratitude to my advisor Prof. Louriel Oliveira Vilarinho for the continuous support of my master study and related research, for his patience, motivation, and immense knowledge. His guidance helped me in all the time of research and writing of this dissertation. I could not have imagined having a better advisor and mentor for my master study.

Besides my advisor, I would like to thank the Federal University of Uberlandia (UFU) and the Faculty of Mechanical Engineering for opportunity to conduct this course. Also to “CAPES” for the financial support in providing scholarship for development this work.

And have to thank all the wonderful people in Brazil, family and friends of Iran, our welding laboratory group (LAPRASOLDA), etc. who have helped me enormously. Actually I would never have been able to finish my dissertation without the guidance, kindness and help of these peoples.

Finally I am grateful to the Nature for the good health, wellbeing and happiness that were necessary to complete this dissertation.

HAMED, A. K. **METAL TRANSFER MAPPING FOR FCAW PROCESS BY USING NEAR-INFRARED FILMING.** 2016. 87p. Master Dissertation, Federal University of Uberlandia, MG, Brazil.

Abstract

In the Flux Cored Arc Welding (FCAW) process, the transfer of filler metal (metal transfer modes) to the base material to accomplish the weld bead determines the weld quality and therefore studies of such phenomena is demanded. Thus, in this work, the metal transfer through the FCAW process is investigated by filming the phenomena with the assist of near infrared visualization. During the literature survey, it was found that this technic has not been used so far for analyzing the FCAW process. It must be pointed out that the radiation emitted from the weld arc, fumes and particles (spattering) in this process represent a barrier for these studies based in the process visualization. The monitoring of metal transfer for FCAW process was carried out within the operational envelope of voltage and wire feed speed with the electrode E71T-1 (1.2 mm diameter) and Ar+25%CO₂ as a shielding gas. A local developed near infrared filming with frame rate of 300 Hz was employed for metal transfer visualization in order to contribute to a better understanding of this process and evaluating characteristics of metal transfer, unlike previous studies, which used shadowgraph technique. It can clearly be seen how the droplet is created and transferred in this process and also identify the different modes of metal transfer by changing the parameters of voltage and wire feed speed in metal transfer maps. The final result of this study is the metal transfer mode maps, which establish suitable conditions and provide the basis for developing arc control strategies for the FCAW process.

Keywords: Flux cored arc welding, Metal transfer modes, Vision systems in welding, Arc length.

HAMED, A. K. **MAPEAMENTO DA TRANSFERÊNCIA METÁLICA PARA PROCESSO FCAW UTILIZANDO FILMAGEM POR INFRAVERMELHO PRÓXIMO.** 2016. 87f. Dissertação de Mestrado, Universidade Federal de Uberlândia, Uberlândia.

Resumo

No processo Eletrodo Tubular (Flux Cored Arc Welding – FCAW), a transferência do metal de adição (transferência metálica) para o material de base, de forma a obter o cordão de solda, determina a qualidade da solda e, portanto, estudos sobre este fenômeno são demandados. Assim, neste trabalho, a transferência metálica durante o processo FCAW é investigada filmando-se esse fenômeno com o auxílio de visualização por infravermelho próximo. Durante a revisão da literatura, não se encontrou outros trabalhos que utilizassem tal metodologia. Deve-se ressaltar que a radiação emitida pelo arco, fumos e partículas (respingos) durante o processo dificulta a visualização do processo. O monitoramento da transferência metálica do processo FCAW foi realizado dentro do envelope de trabalho de tensão e velocidade de alimentação do eletrodo E71T-1 (1,2 mm de diâmetro) e Ar+25%CO₂, como gás de proteção. Foi utilizado um sistema de visualização por infravermelho próximo desenvolvido localmente a uma taxa de 300 quadros por segundo, de forma a contribuir para o entendimento do processo e avaliação das características da transferência metálica, diferentemente de outros processos, os quais utilizaram a técnica de perfilografia (shadowgrafia). Foi possível observar a formação e transferência da gota durante o processo e identificar os diferentes modos de transferência ao se variar os parâmetros de tensão e velocidade de alimentação nos mapas de transferência. Os resultados finais do trabalho são os mapas de transferência, os quais estabelecem condições adequadas e fundam as bases para o desenvolvimento de estratégias de controle do arco para o processo FCAW.

Palavras-chave: Eletrodo Tubular, Modos de transferência metálica, Sistemas de visão na soldagem, Comprimento do arco.

حامد علینژاد کردی. نقشه انتقال فلز در فرایند جوشکاری زیر پودری با فیلمبرداری از طریق پرتوهای مادون قرمز نزدیک. 2016. 87ص. پایان نامه کارشناسی ارشد، دانشگاه فدرال آبرلانندیا، آبرلانندیا.

چکیده

در فرآیند جوشکاری توپودری، انتقال فلز پرکننده (حالت های انتقال فلز) به قطعه کار یا فلز پایه برای تشکیل مهره یا گرده جوش تعیین کننده کیفیت جوش میباشد که به همین راستا مطالعات بیشتر در مورد این پدیده را تقاضا میکند. براین اساس در این پایان نامه، انتقال فلز در فرآیند جوشکاری توپودری با فیلم برداری از پدیده توسط پرتوهای مادون قرمز نزدیک مورد بررسی قرار گرفته است. با توجه به مطالعات و مرور ادبیات گذشته مشخص شده است که این تکنیک تا به حال برای تجزیه و تحلیل فرآیند توپودری استفاده نشده است. باید اشاره کرد که تابش ساطع شده از قوس جوش، دود و ذرات موجود در این فرآیند نشان دهنده یک مانع برای مطالعه در روند تجسم است. نظارت بر انتقال فلز در فرآیند جوشکاری توپودری در این پایان نامه با نرخ های عملیاتی مشخص از ولتاژ و سرعت تغذیه با الکتروود E71T-1 (1.2 میلیمتر قطر) و مخلوطی از 75 درصد آرگون و 25 درصد دی اکسید کربن به عنوان گاز محافظ انجام شده است. بدین منظور از یک سیستم نمایش پرتوهای مادون قرمز نزدیک توسعه یافته محلی با نرخ فریم 300 هرتز برای نظارت بر انتقال فلز به منظور کمک به درک بهتر این فرآیند و ویژگی های ارزیابی انتقال فلز بر خلاف روش قبلی که تکنیک شادوگرافی بوده است، به کار گرفته شده است. سر انجام، عملاً به وضوح دیده خواهد شد که چگونه قطره ایجاد شده و انتقال فلز در این فرایند انجام میگردد و همچنین حالت های مختلف انتقال فلز با تغییر پارامترهای ولتاژ و نرخ تغذیه الکتروود قابل تشخیص خواهد بود. نتیجه نهایی این پایان نامه نقشه حالت های مختلف انتقال فلز است که باعث ایجاد شرایط مناسب و ارائه مبنایی برای توسعه استراتژی های کنترل قوس الکتریکی فرایند جوشکاری توپودری میشود.

کلمات کلیدی: فرایند جوشکاری توپودری، حالت های انتقال فلز، سیستم نظارت و دید در جوشکاری، طول قوس.

LIST OF FIGURES

Figure 2.1.1: Schematic view of the FCAW process [5].....	5
Figure 2.1.2: Schematic view of the SS-FCAW process [7]	6
Figure 2.1.3: Schematic view of the GS-FCAW process [7]	7
Figure 2.2.1: The basic manufacturing Inner shield Electrodes steps [6]	9
Figure 2.2.2: Cored wire manufacturing process (Putting the flux in the cored wire) [7]	9
Figure 2.3.1: IIW classification of metal transfer depicted in an arc voltage and welding current diagram [12]	12
Figure 2.3.2: Fundamental transfer modes. U (I) diagram based on the classification [9]	13
Figure 2.3.3: Image sequence captured during metal transfer of a rutile wire for a current around 160A. (a) Welding with 100% CO ₂ (b) Welding with 75% Ar-25% CO ₂ [2]	15
Figure 2.3.4: Image sequence captured during metal transfer of a rutile wire for a current around 200 A. (a) Welding with 100% CO ₂ (b) Welding with 75% Ar-25% CO ₂ [2]	16
Figure 2.3.5: Metal transfer map for welding with shielding gas containing Ar+2% O ₂ [3]	17
Figure 2.3.6: Metal transfer map for welding with shielding gas containing Ar+5% O ₂ [3]	17
Figure 2.4.1: visualization of metal transfer by shadowgraph technique [18].....	18
Figure 2.4.2: visualization of molten metal by indirect illumination [19]	19
Figure 2.4.3: Images obtained with filter at 950 nm in the study of the MIG/MAG process [21].....	19
Figure 2.4.4: Principle of spectrum filtering [19]	20
Figure 2.4.5: Set the exposure time of the camera to minimize the power applied to the pulsed laser compared to the continuous nature of the arc radiation [4]	20
Figure 2.4.6: Viewing system with high-power laser diodes in near infrared for TIG (left) and MIG/MAG welding (center and right) [17, 4]	21
Figure 3.1.1: Welding power supply (IMC MTE Digitec 300).....	24
Figure 3.1.2: Electrode wire feeding system (IMC STA-20)	25
Figure 3.1.3: A) Knurled V groove rolls for FCAW B) The 4 rollers set up wire feeder	26
Figure 3.1.4: Welding torch, steel contact tip and shielding nozzle	27
Figure 3.1.5: Welding table	27
Figure 3.1.6: A) Signal Conditioner; B) Acquisition board; C) Hall Effect sensor; D) LabVIEW programming software; E) OriginPro 9.0 application.	29
Figure 3.1.7: Clamping system for supporting of plate during the welding process.	29
Figure 3.1.8: Source of Infrared (ViaSolda)	30
Figure 3.1.9: High speed digital camera (HiSpec 5) and filter	31

Figure 3.1.10: HiSpec 5 home Screen Software	31
Figure 3.2.1: A) Flowmeter, B) regulator.....	33
Figure 3.2.2: FCAW Electrode Classification (AWS Specification- A5.20)	34
Figure 3.2.3: A) horizontal bandsaw machine B) surface grinder machine	37
Figure 3.3.1: A diagram showing the contact tip position relative to the shielding nozzle used during welding.....	38
Figure 3.3.2: Travel angle. A) Forehand, B) Perpendicular, and C) Backhand angles [4]	39
Figure 3.3.3: work angle [27].....	39
Figure 3.3.4: Schematic of 3-dimensional imagery technic positioning	42
Figure 3.3.5: Observation of different arc lengths.....	43
Figure 3.3.6: Schematic view to measuring of arc length in different situation	44
Figure 4.1: Observed and categorized metal-transfer modes during FCAW	47
Figure 4.1.1: Voltage and current signals for a short circuit metal transfer-(Run 39)	50
Figure 4.1.2: Image sequence captured during FCAW in a short circuit transfer mode- (Run 39).....	51
Figure 4.1.3: Voltage and current signals for a short circuit and free flight metal transfer-(Run 28) ...	52
Figure 4.1.4: Schematic electrode positioning for A) without buried and B) with buried metal transfer type	53
Figure 4.1.5: Image sequence captured during FCAW in a short circuit and free flight mode without buried (SC-FF-WOB)-(Run 48).....	54
Figure 4.1.6: Image sequence captured during FCAW in a short circuit and free flight mode with buried (SC-FF-WB)-(Run 71)	56
Figure 4.1.7: Voltage and current signals for a free flight metal transfer-(Run 55)	57
Figure 4.1.8: Schematic of metal transfer for A) Split type and B) Conjunct	58
Figure 4.1.9: Image sequence captured during FCAW in a free flight mode without buried in conjunct type (FF-WOB-CO)-(Run 46)	59
Figure 4.1.10: Image sequence captured during FCAW in a free flight mode without buried in split type (FF-WOB-SPL)-(Run 102).....	61
Figure 4.1.11: Image sequence captured during FCAW in a free flight mode with buried (FF-WB) A) Run 88 B) Run 79	62
Figure 4.2.1: Map of metal transfer modes in FCAW process as a function of mean welding voltage and wire feed speed.....	64
Figure 4.2.2: Map of metal transfer modes in FCAW process as a function of mean arc length and mean current	64
Figure 4.2.3: Arc length variation observed in the images for different runs	65

Figure 5.1: Schematic map of the metal transfer modes in FCAW process as a function of wire feed speed and voltage (L_a is the arc length)67

Figure 6.1: Schematic of metal transfer in MIG/MAG laser process. A) With buried B) Without buried69

LIST OF TABLES

Table 2.1: Summary of metal transfer mode evolution [13]	11
Table 2.2: Proposed classification of metal transfer in GMA processes [9]	14
Table 2.3: Characteristics of LED diodes and laser diodes [16]	21
Table 2.4: Characteristics of the SPL PL90_3 pulsed laser diode [22]	22
Table 3.1: Nominal chemical composition of AISI 1020 steel	35
Table 3.2: Welding parameters to find plate thickness	36
Table 3.3: Experimental design showing the test numbering (from 1 to 108)	40
Table 4.1: Applicable and non-applicable tests number (input values to power source)	48
Table 4.2: Set value and monitoring results for short circuit mode	49
Table 4.3: Set value and monitoring results for short circuit and free flight without buried (SC-FF-WOB)	53
Table 4.4: Set value and monitoring results for short circuit and free flight with buried (SC-FF-WB) ..	55
Table 4.5: Set value and monitoring results for free flight metal transfer without buried in conjunct type (FF-WOB-CO)	59
Table 4.6: Set value and monitoring results for free flight metal transfer without buried in split type (FF-WOB-SPL)	60
Table 4.7: Set value and monitoring results for free flight metal transfer with buried (FF-WB).	62

LIST OF SYMBOLS

AWS	- American Welding Society
GMAW	- Gas Metal Arc Welding
FCAW	- Flux Cored Arc Welding
MIG	- Metal Inert Gas
MAG	- Metal Active Gas
GS-FCAW	- Gas Shielded Flux Cored Arc Welding
SS-FCAW	- Self Shielded Flux Cored Arc Welding
SAW	- Submerged Arc Welding
TIG	- Tungsten Inert Gas

.....

AC	- Alternating Current
DC	- Direct Current
DCEP	- Direct Current Electrode Positive
DCEN	- Direct Current Electrode Negative
I	- Current
I_m	- Mean Current
I_{rms}	- Effective Current
U	- Voltage
U_m	- Mean Voltage
U_{rms}	- Effective Voltage
U_r	- Reference Voltage

.....

CTWD	- Contact Tip to Work Distance
ESO	- Electrical Stick Out
L_a	- Arc Length
MR	- Melting Rate

.....

CO	- Conjunct
GL	- Globular

RE	- Repulsion
FF	- Free Flight
SC	- Short Circuit
SP	- Spray
SPE	- Spray elongation
SPL	- Split
WB	- With Buried
WOB	- With Out Buried

.....

ABNT	- Brazilian Association of Technical Standards
AISI	- American Iron and Steel Institute
DAQ	- Data transient Acquisition system
IPM	- Inches per Minute
NIR	- Nera Infrared

.....

h	- Plate thickness (mm)
h_{crit}	- The critical thickness (mm)
H	- Welding energy (kJ/mm)
H_L	- Heat input (kJ/mm)
W_s	- Welding Speed (cm/min)
WFS	- Wire Feed Speed (m/min)
C	- Specific heat of the base material (J/g °C)
T_0	- Initial temperature or preheating (°C)
T_p	- Peak temperature (°C)
T_f	- Melting temperature of base metal (°C)
\bar{T}	- Relative thickness
ρ	- Density of base material (g/cm ³)
\emptyset	- Electorde diameter (mm)

Table of contents

Abstract	V
Resumo.....	VI
چکیده.....	VII
LIST OF FIGURES.....	VIII
LIST OF TABLES	XI
LIST OF SYMBOLS	XII
CHAPTER I.....	1
INTRODUCTION	1
CHAPTER II.....	4
LITERATURE REVIEW	4
2.1 Fundamentals of Flux Cored Arc Welding process (FCAW):	4
2.2 Manufacturing Inner shield Electrodes:	8
2.3 Definition of metal transfer modes	9
2.4 Vision System in Welding.....	17
CHAPTER III.....	23
EXPRIMENTAL EQUIPMENT, MATERIALS AND METHODS	23
3.1 Experimental Equipment	23
3.1.1 Welding power supply:	24
3.1.2 Electrode wire feeding system:	25
3.1.3 Welding torch:.....	26
3.1.4 Coordinate welding table:.....	27
3.1.5 Electrical data transient Acquisition system (DAQ):	28
3.1.6 Holding system for plates:	29
3.1.7 Digital High Speed Camera and Near-infrared vision system:	30
3.2 Material and Consumable.....	32
3.2.1 The shielding gas:	32
3.2.2 Filler metal or electrode:	33
3.2.3 Metal base and workpiece:.....	34
3.3 Methodology.....	38
3.3.1 Contact Tip to Work Distance (CTWD).....	38
3.3.2 Torch Angles.....	38

3.3.3 Voltage, Wire Feed Speed and Travel speed,.....	40
3.3.4 Position of systems form interest area	41
3.3.5 Measurement of the arc length	42
3.3.6 Turning on the ViaSolda	44
3.3.7 Drawing the metal transfer maps.....	44
3.3.8 Preparation of welding environment	44
3.3.9 Welding Experimental Procedure.....	45
CHAPTER IV.....	46
RESULTS AND DISCUSSION	46
4.1 Metal transfer modes	46
4.1.1: Short Circuit (SC):	48
4.1.2 Short circuit and free flight (transition area):	51
4.1.2.1 Short circuit and free flight without buried (SC-FF-WOB):.....	53
4.1.2.2 Short circuit and free flight with buried (SC-FF-WB):	54
4.1.3 Free Flight:	56
4.1.3.1 Free flight without buried in conjunct type (FF-WOB-CO).....	58
4.1.3.2 Free flight without buried in split type (FF-WOB-SPL)	60
4.1.3.3 Free flight with buried (FF-WB)	61
4.2 Presentation of metal transfer maps	63
CHAPTER V.....	66
Conclusion	66
CHAPTER VI.....	68
Improvements – Future Work	68
CHAPTER VII.....	70
References.....	70

CHAPTER I

INTRODUCTION

Gas Metal Arc Welding (GMAW) process has been in use since the early 1920's. Experiments at that time showed a significant improvement of weld metal properties when the arc and molten weld metal were protected from atmospheric contamination. However, the development of coated electrodes in the late 1920's reduced the interest in gas shielded methods.

Not until the early 1940's, with the introduction of the commercially-accepted gas tungsten arc welding process, it did there become a renewed interest in these gas-shielded methods. Later in that same decade, the gas metal arc welding process was successfully commercialized. Argon and helium were the two primary shielding gases at that time.

Research work conducted on manual coated electrode welds dealt with an analysis of the gas produced in the disintegration of electrode coatings. Results of this analysis showed that the predominant gas given off by electrode coatings was CO₂. This discovery led quickly to the use of CO₂ for shielding of the gas metal arc process when used on carbon steels. Although early experiments with CO₂ as a shielding gas were unsuccessful, techniques were finally developed which permitted its use. Carbon dioxide shielded GMAW became commercially available in the mid-1950's.

About that same time, the CO₂ shielding was combined with a flux-containing tubular electrode which overcame many of the problems encountered previously. Operating characteristics were improved by the addition of the core materials and weld quality was improved by eliminating atmospheric contamination.

Flux cored arc welding (FCAW) process was introduced publicly at the AWS Exposition held at Buffalo, New York, in May 1954. The electrodes and equipment were refined and introduced in essentially the present form in 1957. The process is being continually improved. Power sources and wire feeders are now greatly simplified and more dependable than their predecessors. The new guns are lightweight and rugged. Electrodes are undergoing continuous improvement. Alloy electrodes and small diameter electrodes down to 0.035 in. (0.9 mm) are some of the later advances [1].

The FCAW process is currently one of the most widely used arc welding process in industry. Benefits such as high production rates, high weld quality, ease of automation, and the ability to weld many metals make it attractive to manufacturers. One of the unique characteristics in this process is the way molten metal is transferred across the arc. The transfer of metal from the electrode to the workpiece influences penetration, bead morphology, fume generation, process stability, and spatter. Metal transfer is controlled by several parameters, including current, voltage, polarity, electrode extension shielding gas composition, and electrode diameter.

The use of low- or high-speed cameras can provide different information that is useful to researchers, which is not possible to obtain with the usual monitoring of electrical signals such as current or voltage. In welding processes, vision can supply information in inspection and welded joint's quality, in the parameters' monitoring, in trajectory correction and even, finally, in the study of the phenomena involved in the process. Metal transfer can be described as the transport of molten droplets from the tip of a consumable electrode to the weld pool. According to the size and transfer characteristics of the molten droplets, different types of transfer modes can be defined. Behavior of a molten pool and metal transfer are closely related to the welding status and weld appearance. In FCAW process like as other process, for applications where the precision is critical, the metal transfer process needs to be monitored and controlled to control the diameter, trajectory, transfer type and transfer rate of the droplet of liquid metal by some imaging technique. Since, it is difficult to directly observe and measure the morphology of a molten pool and metal transfer due to its quick and dynamic variation so should be utilized a high speed imagery technique. Some researchers [2, 3] utilized shadowgraph's technique for monitoring of metal transfer for this process. This technique can provide photos of droplet during the welding process, but lack the ability to monitor the weld pool and also because of the radiation emitted from the weld arc, fume and gases that represents a barrier for this process and could reduce the quality of pictures of metal transfer in FCAW process. One approach to solve such problems is filtering

the radiation of welding arc by using near infrared filming. Also the direct visualization in this study has ability to monitor the weld pool. It takes advantage of the specular surface of a molten weld pool by reflecting of lights from the weld pool surface. Also the electrical signals through the arc is one sensing strategy for an intelligent welding control system which monitored in this study. A local developed near infrared filming with frame rate of 300 Hz was employed by Mota [4] for metal transfer visualization in order to contribute to a better understanding of this process and evaluating characteristics of metal transfer, unlike previous studies, which used shadowgraph technique.

Therefore, the objective of this work is to assess the metal transfer during the FCAW process by filming the phenomena with the assist of near infrared visualization within the operational envelope of voltage and wire feed speed with the electrode E71T-1 (1.2 mm diameter) and Ar+25%CO₂ as a shielding gas.

CHAPTER II

LITERATURE REVIEW

This chapter provides an overview of previous research on knowledge sharing and intranets. It introduces the framework for the case study that comprises the main focus of the research described in this dissertation.

This literature review aims to gather information about the welding process of Flux Cored Arc Welding (FCAW), mode of metal transfer on that, vision system in welding and serve as a technical and scientific basis to understand the basic principles involved in that process, the basis for discussion of results.

2.1 Fundamentals of Flux Cored Arc Welding process (FCAW):

Flux Cored Arc Welding is an arc welding process that uses an arc between a continuous filler metal electrode and the weld pool. The process is used with shielding from a flux contained within the tubular electrode, with or without additional shielding from an externally supplied gas, and without the application of pressure (Figure 2.1.1).

The flux cored electrode is a composite tubular filler metal electrode consisting of a metal sheath and a core of various powdered materials. During welding an extensive slag cover is produced on the face of a weld bead [1].

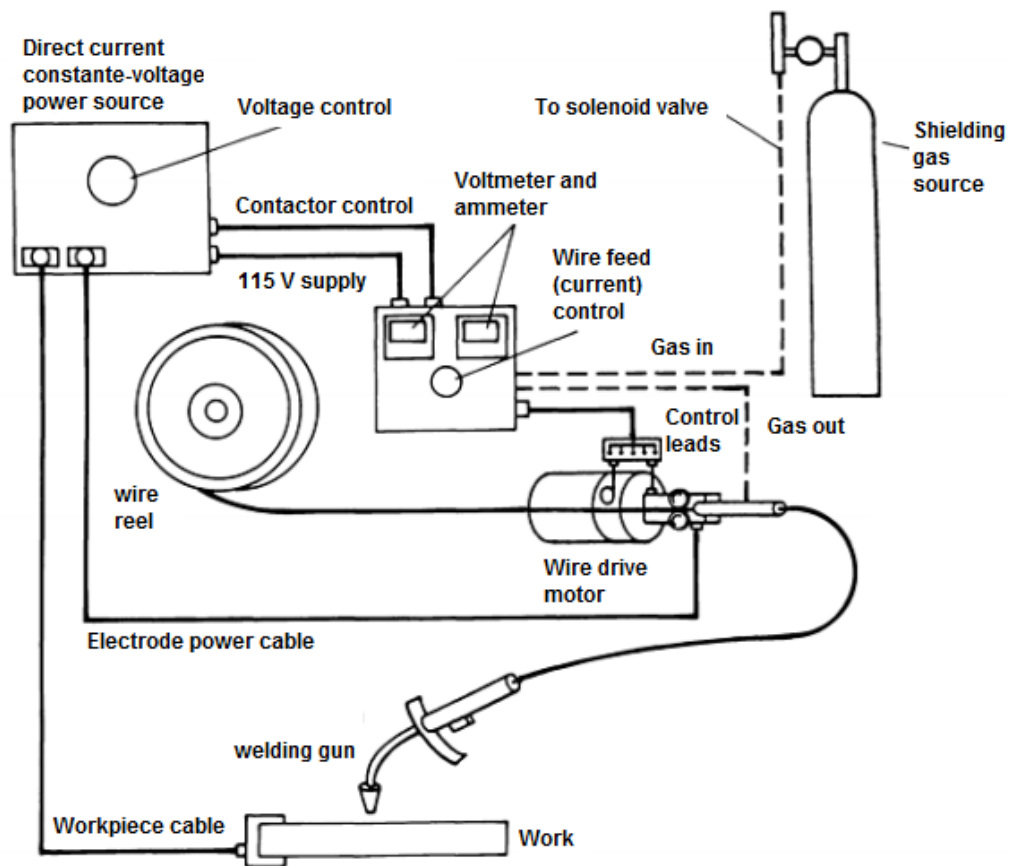


Figure 2.1.1: Schematic view of the FCAW process [5]

A fundamental principle of arc welding is that the arc and molten weld metal must be protected from exposure to the atmosphere. Otherwise nitrogen and oxygen (approximately 99% of air's constituents) will react with the arc and will be absorbed into the molten metal. Before the puddle solidifies, the absorbed gases may not completely escape. The result is porosity in the weld metal and typically a significant decrease in the weld's mechanical properties, particularly toughness [6].

To achieve protection from the atmosphere, arc welding processes use either a slag system and/or an external shielding gas system. With a slag system, elements inside the electrode react with air, produce their own shielding gas and form a protective slag on the surface of the weld. While arc characteristics may be slightly less desirable (more spatter, harsher arc, etc.), these processes are very resistant to interference with the arc from surrounding air flow (wind, fans, etc.). On the other hand, external shielding gas systems deliver a particular gas or gas mix out from the end of the welding gun, where it surrounds the arc and weld pool, displacing the air and acting as a protective barrier for a second or two until the puddle solidifies. This gas environment generally improves the arc characteristics

and resulting operator appeal (less spatter, smoother arc, etc.). However, these processes are very sensitive to arc interference and contamination from surrounding air flow [6].

The Flux-Cored Arc Welding (FCAW) process uses a continuously fed electrode to supply filler metal to the arc. The electrode is not solid, but rather is tubular with flux inside of it. This process is then divided into two fundamentally different sub-processes; the Self-Shielded Flux-Cored Arc Welding (SS-FCAW) process and the Gas-Shielded Flux-Cored Arc Welding (GS-FCAW) process. While electrodes for both sub processes produce a slag covering over the weld, the method in which they protect the arc from the surrounding atmosphere is quite different. With the SS-FCAW process, reactionary agents necessary to shield the arc and cleanse the molten weld pool are placed inside the tube. No additional shielding is required (Figure 2.1.2). Whereas the GS-FCAW process has a different type of flux core system and relies completely on an external shielding gas for atmospheric protection (Figure 2.1.3).

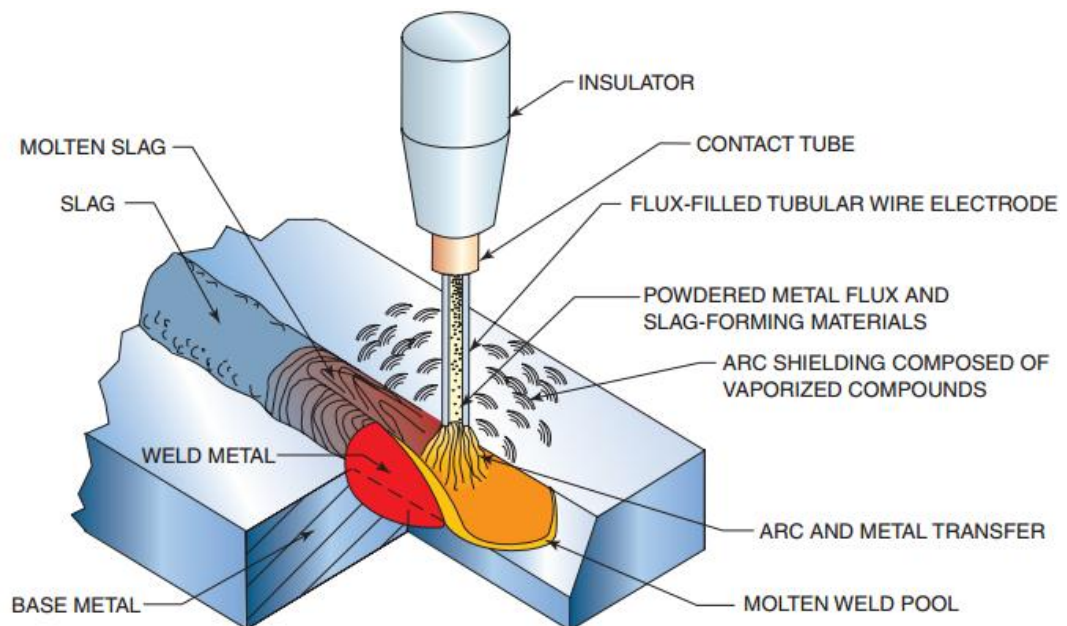


Figure 2.1.2: Schematic view of the SS-FCAW process [7]

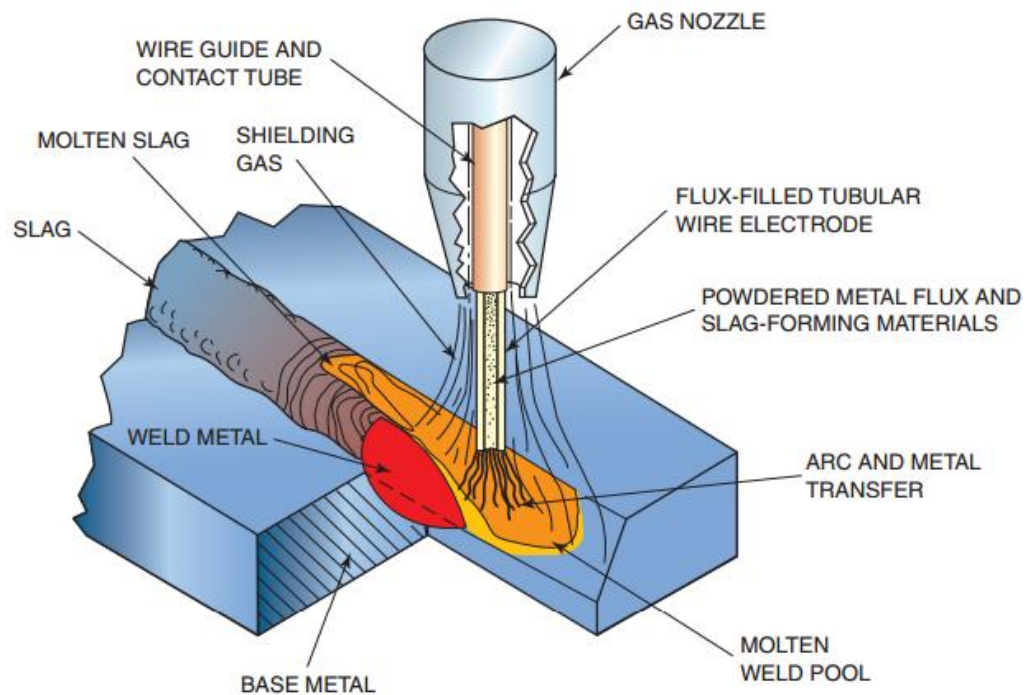


Figure 2.1.3: Schematic view of the GS-FCAW process [7]

Like any process, welding with tubular electrode has its advantages and limitations. For your application, it must be analyzed, along with the practical results, to see, it becomes convenient or not. The benefits of FCAW process are related to its:

- Productivity related to the use of continuous wires;
- Metallurgical benefits from the internal wire flow;
- Aid the slag in the form and appearance of the weld bead.
- High quality of the deposited metal;
- Excellent weld appearance (uniform solder);
- Welding various types of steel and in large thickness ranges;
- Easy operation due to the high ease of mechanization;
- High deposition rate due to high current density;
- Relatively high efficiency of deposition;
- Requires less cleaning than in GMAW (More deoxidizer within the flux);
- High tolerance for contaminants that can cause cracks;
- High productivity.

On the other hand, the process limitations are related to:

- Limited to weld ferrous and alloy nickel-based;
- Slag removal need;
- The equipment is more expensive compared to that used for the SMAW welding process;
- Outdoor welding Restriction (only for FCAW welding with shielding gas);
- The wire feeder and the power source must be close to the workplace;
- It generates more fumes than the GMAW and SAW processes.

2.2 Manufacturing Inner shield Electrodes:

The process of drawing down and adding flux to the inside of an electrode is much more complex than drawing down solid electrodes (i.e. MIG wire). Flux-cored electrodes are considered “fabricated” wires. The basic manufacturing steps include:

1. Flux-cored electrodes start off in one of two forms of raw steel, round “green rod” or flat “strip”.
2. The steel is drawn down and rolled into a “U” shape.
3. Flux ingredients are then uniformly poured into the U shaped tube. Monitoring equipment ensures that 100% of the electrode has the proper fill rate.
4. The electrode is then rolled together with a tight seam, which is either a butt or lap seam. The outer steel tube is called the “sheath” or “jacket” and the inner portion is the “flux core”.
5. The electrode is then drawn down to its final diameter and a lubricant is applied to the surface. This lubricant, aids in wire feeding and acts as a rust inhibitor. Cored electrodes are not copper coated¹ like solid electrodes (i.e. TIG, MIG or submerged arc electrodes), in which the copper is attached via an acid bath and chemical reaction. If it were attempted with cored electrodes, the acid solution would seep through the seam and contaminate the flux [6].

¹ The exception is seamless flux-cored electrodes, which do have an external copper coating. This is a relatively new manufacturing process with few products in the welding market.

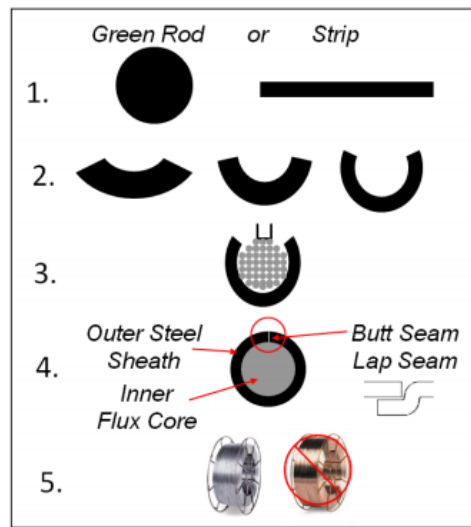


Figure 2.2.1: The basic manufacturing Inner shield Electrodes steps [6]

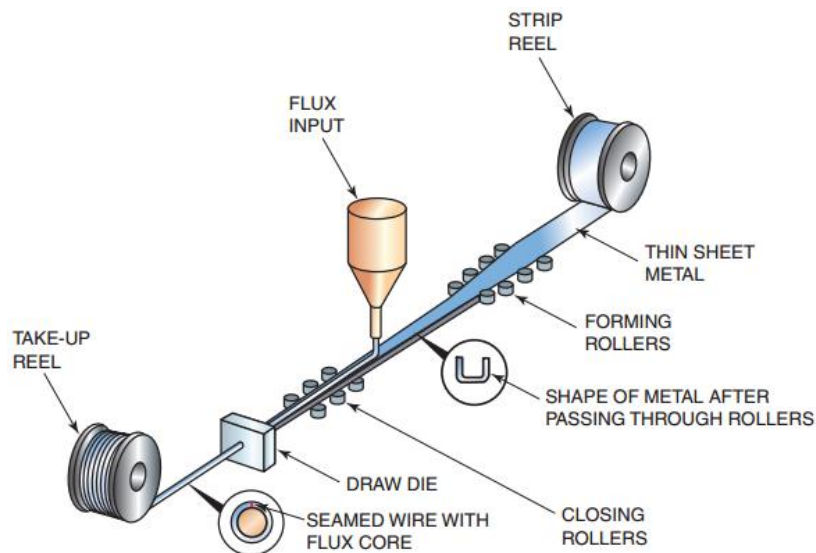


Figure 2.2.2: Cored wire manufacturing process (Putting the flux in the cored wire) [7]

2.3 Definition of metal transfer modes

One of the main factors that influence obtaining a good quality weld is how the material is transferred (deposited) from the electrode (filler material) to the weld pool, in other word, the metal transfer mode. Features such as the process stability in the various positions, spatter level, wettability of the metal base, and geometric aspects of the bead surface are directly related to the type of metal transfer.

The mode of metal transfer is determined by many other factors:

- Base Metal Type;
- Filler Metal Composition;
- Electrode Diameter;
- Polarity;
- Arc Current;
- Arc Voltage/Arc Length;
- Shielding Gas Composition;
- Welding Position;
- CTWD (contact tip to work distance)

In metal transfer, if the wire feed rate be balanced by its fusion rate, the process wrought of stable shape and keeps going. A failure in this swing resulted in the arc extinction, or short circuit or excessive growth of the arc. The relationship between the rate of melting and the current is given and widely presented in the literatures as:

$$MR = \alpha I_m + \beta LI_{rms}^2 \quad \text{Equation 2-1}$$

Where MR is melting rate, α and β are constants associated with the gas protection, polarity and diameter and material of electrode, I is current and L is the electrode extension.

Following the first classification of arc types in 1976 [8], several further classifications have been proposed. Short circuit, globular, and spray are the three major classifications of metal transfer types by the American Welding Society (AWS) [9]. The International Institute of Welding (IIW), in 1984, divided spray types into the three categories: (i) drop spray or projected spray, (ii) rotating spray, and (iii) streaming spray [10]. Norrish [11] and then Ponomarev et al [12] modified this categorization. Utilization of digital control of power sources has led to many improvements in arc control, especially in welding with short circuit and pulsed mode of metal transfer. Digital control increases the reaction speed of the power source inverter and the use of sophisticated software makes it possible to directly influence the arc [9]. Table 2.1 summarizes the attempt to classify metal transfer [13].

Table 2.1: Summary of metal transfer mode evolution [13]

Classification basis	Description	References
Droplet transfer	Free flight, short circuiting. A slag mode is defined for other arc welding (SAW)	IIW (1976), referred by Lancaster (1984) as Anon
Droplet transfer and droplet size	Categorization by level of current and drop size current: moderate current (globular), relatively high current (spray), high current (stream), very high current (rotating)	Lancaster (1984)
Associated transfer mechanism	Mechanisms: (1) natural metal transfer, (2) controlled transfer techniques, and (3) extended operating mode techniques	Norrish (2003)
Transfer mechanism and labelled with alphabet letters	Suggested confining the classification to natural and controlled transfer modes. In addition, these authors proposed an extra fixed alphabetic label for each 'fundamental' metal transfer mode (A, short circuiting; B, globular; C, pulsed; D, spray; and E, rotating)	Lucas et al. (2005)
Current range, sketch illustration, and type of consumable electrode	Droplet transfer during GMA welding with solid wire and FCW has been observed in detail and the transfer	Izutani et al. (2006)
Sketch illustration of the mechanisms and an alphabetic associated with number classification	The range of current is provided for each transfer mode A, short circuiting; B, globular; C, spray. Similar approach using alphanumeric Labels (A, B1, B2, C1, C2, and C3). The controlled processes classification and defined two types of controlling processes, either simple controlled processes or real-time controlled processes	Iordachescu and Quintino (2008)
Metal transfer-natural transfer, controlled transfer and mixed mode transfer, oriented to scientific personnel	Metal transfers are illustrated by a sequence of droplet transfer. Corresponding main forces governing the metal transfer are indicated for each case. Metal transfer modes are categorized in a flow chart: natural transfer, controlled, and interchangeable transfer	Scotti et al. (2012)

According to Wang et al [14] arc modes are related to arc voltage and the level of current. By changing these two parameters, the modes of the arc can be changed. With small current, the droplet does not form until it touches the weld pool; this mode of arc is a so-called short circuit. The metal transfer mode changes to a globular when the current is increased so that a small electromagnetic force is generated. In a globular mode, the diameter of the droplet is bigger than the electrode and the droplet is formed by the gravitational force. By further increasing the current, the type of transfer changes to a projected spray mode, then a streaming mode, and finally a rotating mode. The different types of metal transfer can be shown in diagrams of arc voltage and current.

As an illustration of the influence of current, voltage, and shielding gas composition, Iordachescu and Quintino in an IIW meeting in 2003 classified arc types on the basis of 'natural transfer modes'. Today, however, due to the use of more developed controllers, natural transfer modes are no longer used as often [9]. Figure 2.3.1 from Ponomarev's study shows metal transfer types as a function of current, voltage, and shielding gas.

The transition current has been an important topic in the type of metal transfer in GMA welding. It sets the limit between globular and spray mode and determines the working conditions of the welding process, as suggested by Ponomarev [12] (Figure 2.3.1). According to Iordachescu and Quintino [9] there could be a second transition current between short circuit and globular, as illustrated in Figure 2.3.2. The aim of the suggestion is to cover both normal spray and projected spray.

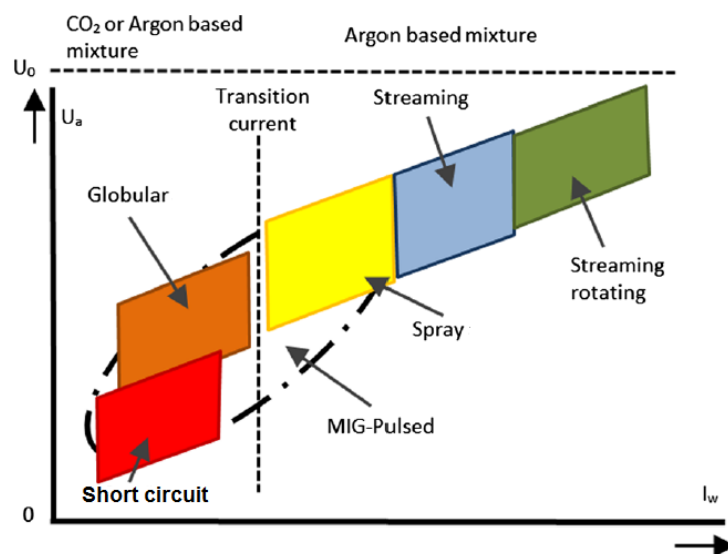


Figure 2.3.1: IIW classification of metal transfer depicted in an arc voltage and welding current diagram [12]

In addition to a second transition current line, the study by Iordachescu and Quintino [9] suggested a new transfer mode classification of the arc in GMAW as a function of the current, voltage, and shielding gas: short circuiting, globular drop, globular repelled, drop spray, streaming, and rotating transfer modes. Figure 2.3.2 illustrates this classification of arcs in GMAW. The first transition current separates the globular with axial droplets and globular with repelled droplets and the second transition current separates the spray and globular fundamental group areas. In addition, the mode of arc changes with increasing welding current and arc voltage. The figure shows that the electric current in short arc transfer is lower than in other types of arcs and that rotating transfer needs a high current.

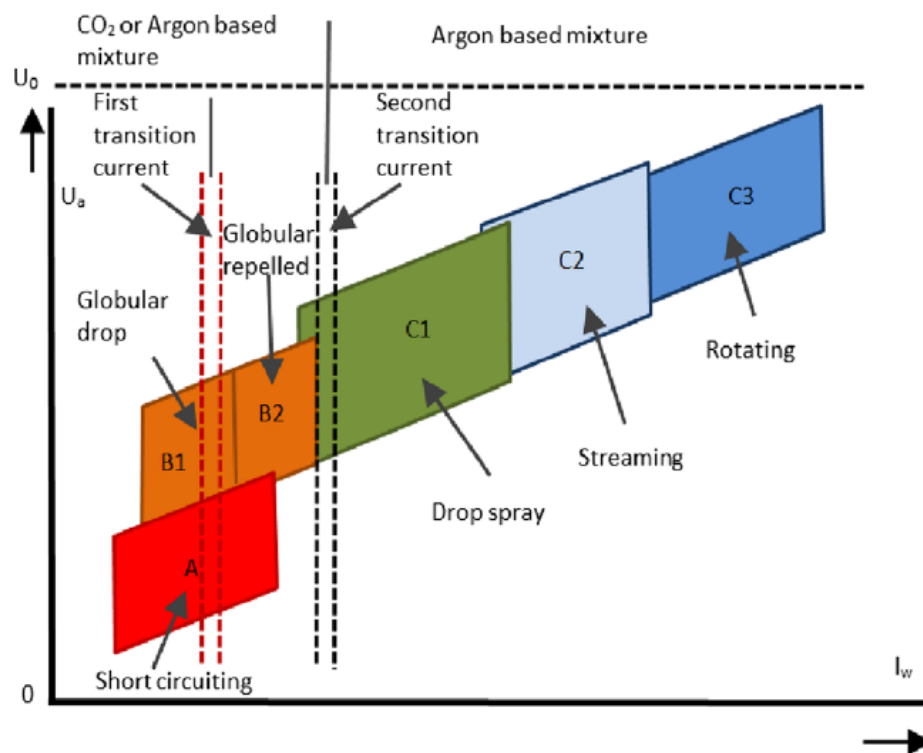


Figure 2.3.2: Fundamental transfer modes. U (I) diagram based on the classification [9]

A metal transfer mode classification structured on the increase of the current and voltage would be welcomed by most of the people active in the field, as it would allow to clearly understanding the relation between the process parameters and metal transfer modes, which are related with arc stability, bead appearance and bead quality.

Based on the main type of forces playing the key-role on the detachment of the molten metal from the wire electrode, three main “categories” of fundamental transfer modes may be defined:




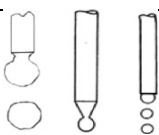

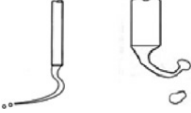
A. Short circuiting—key-role played by the surface tension resultant force.

B. Globular—key-role played by the gravity resultant force.

C. Spray—key-role played by the arc pressure resultant force.

To make the proposed classification simpler, only the level two categories where denominated as fundamental transfer modes, as shown in Table 2.2. This makes the classification simpler, without losing the logic of numbering, both from fundamental point of view (the physics of the transfer) and the technological one (the increasing of the values of the welding parameters). Consequently, the six fundamental transfer modes in the new classification are: A-Short circuiting, B1- Globular drop, B2-Globular repelled, C1-Drop spray, C2-Streaming and C3-Rotating.

Table 2.2: Proposed classification of metal transfer in GMA processes [9]

Proposed denomination (fundamental modes)	Proposed name (fundamental modes)	Sketch	Comment	Correspondent in IIW classification [5]
A	Short circuiting			2.Bridging transfer 2.1Short circuiting
B1	Globular Drop			1. Free flight transfer 1.1 Globular 1.1.1 Drop
B2	Globular Repelled		CO2 GMAW	1. Free flight transfer 1.1 Globular 1.1.2 Repelled
C1	Drop Spray		(projected)	1. Free flight transfer 1.2 Spray 1.2.1 Projected or not applicable, as presented by [8]
C2	Streaming			1. Free flight transfer 1.2 Spray 1.2.2 Streaming
C3	Rotating			1. Free flight transfer 1.2 Spray 1.2.3 Rotating

In FCAW process, form of metal transfer depends primarily on the characteristics of each type of wire flux. According to Norrish [15], for rutile flux-cored wires, these consumables are normally operated in the spray mode where they give smooth non axial transfer. Some of the flux melts to form a slag layer on the on the surface of the droplet, a small amount decomposes to form shielding gases whilst some unmelted flux is transferred to the weld pool where it melts and produces a protective slag blanket. The unmelted flux projects from the tip of wire.

Cícero et al [2] evaluated the metal transfer in tubular wire welding by using a high speed video camera and laser shadowgraphy. Welding tests with different current levels were performed with a rutile tubular wire of 1.2mm diameter, two gas mixtures (100%CO₂ and 75%Ar-25%CO₂) with an electrode stick out of 16mm and an arc length of 3.5mm. Globular metal transfer together with a flux column projecting towards the weld pool was observed for welding current around 160 A for both gas mixtures. A similar result was obtained for higher current levels (around 200 A), however with smaller drop diameter and higher transfer frequency. This effect was more pronounced for the welding trials with 75%Ar-25%CO₂ shielding.

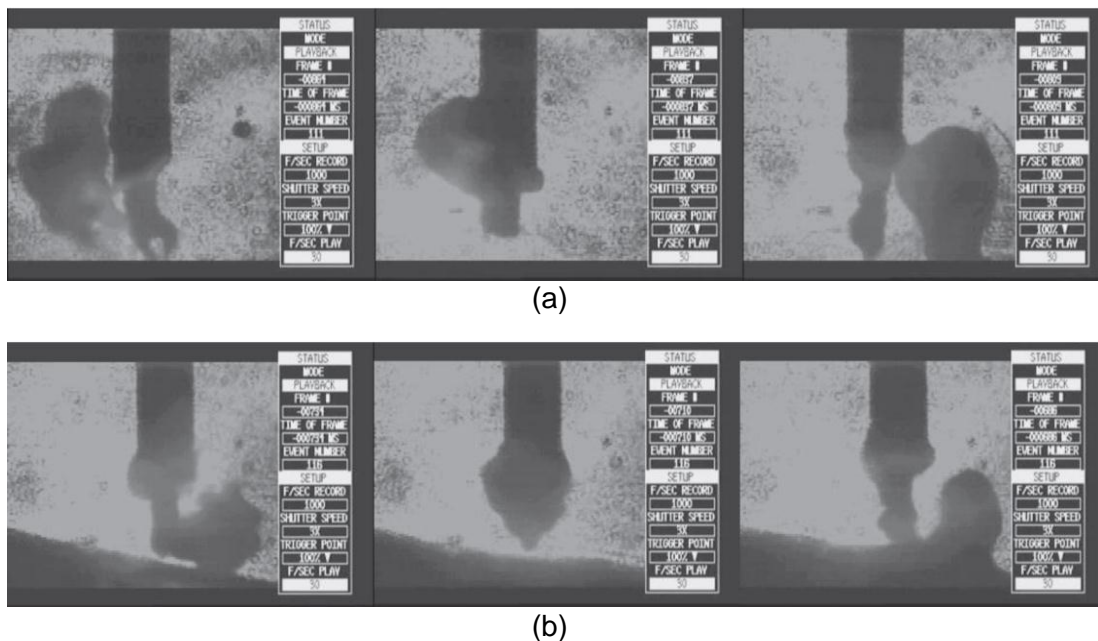


Figure 2.3.3: Image sequence captured during metal transfer of a rutile wire for a current around 160A. (a) Welding with 100% CO₂ (b) Welding with 75% Ar-25% CO₂ [2]

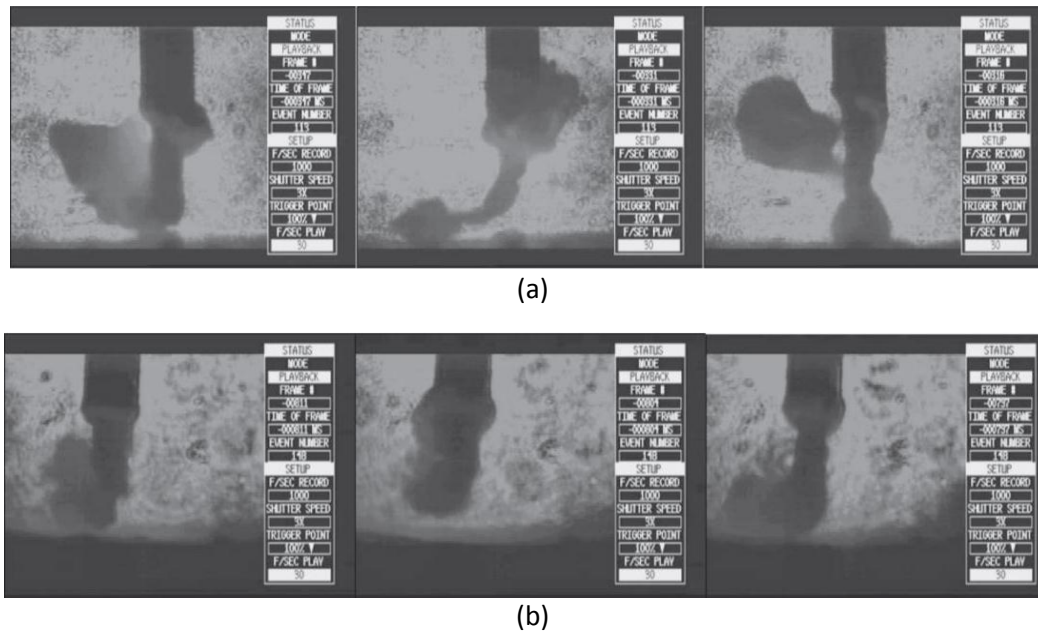


Figure 2.3.4: Image sequence captured during metal transfer of a rutile wire for a current around 200 A. (a) Welding with 100% CO₂ (b) Welding with 75% Ar-25% CO₂ [2]

In 2004, Luz et al [3] used one multi process welding source in the constant voltage mode and positive polarity (DC +) to analyzing the metal transfer of FCAW. The aim of this work was to obtain the metal transfer map of a commercial tubular wire (metal cored wire 409Ti) with a diameter of 1.2 mm and assess the shielding gas influence (Ar+2%O₂ and Ar+5%O₂) on the metal transfer. The contact tip to work distance (CTWD) was maintained at 18 mm, with torch perpendicular to the plate. A high-speed filming system was employed in addition to a laser head and a set of optical filters to provide the image recording of the electrode, droplets and bead shadows (this experimental rig is known as Shadowgraph or Backlight technique).

During the assembly of metal transfer map for the two welding conditions (two types of shielding gas) has been verified occurrence of similar modes which include: globular (GL), short circuit (SC) spray (SP), spray with elongation (SPE), short circuit / repulsion (SC-RE) globular / short circuit / spray (GL-SC-SP), globular / spray (GL-SP) and with spray elongation / spray (SPE-SP). For welding using shielding gas with 2% O₂ it was the presence of mixed-mode short circuit / spray (SC-SP) and short circuit / spray / repulsion (SC-SP-RE). For welding using shielding gas with 5% O₂ there was the spray modes / repulsion (SP-RE) and the repulsion mode (RE). The Figures 2.3.5 and 2.3.6 represent the metal transfer maps for welding with the shielding gas containing Ar+2%O₂ and Ar+5%O₂, respectively. It is observed in these figures distinguish the four areas, in which a dominant

mode (mode pure) acts more strongly. In Region 1 there is the predominance of the globular way, region 2 the short circuit mode region 3 spray mode and the region 4 is spray mode with elongation. Finally, this study makes it clear that metal cored is similar to MIG/MAG.

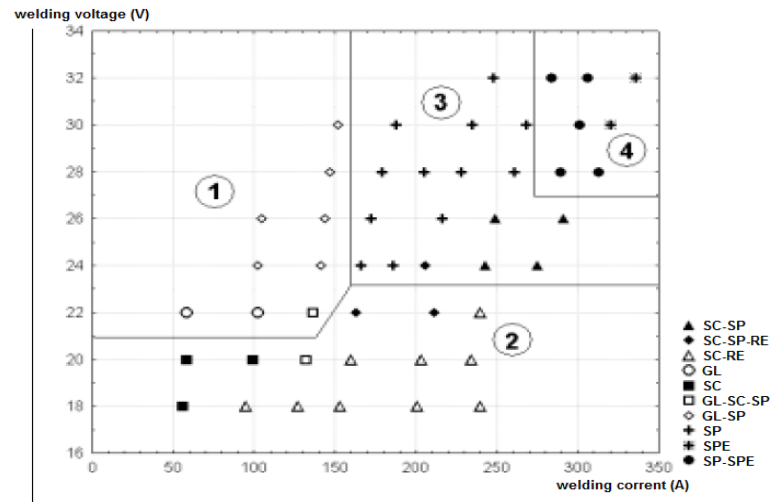


Figure 2.3.5: Metal transfer map for welding with shielding gas containing Ar+2% O₂ [3]

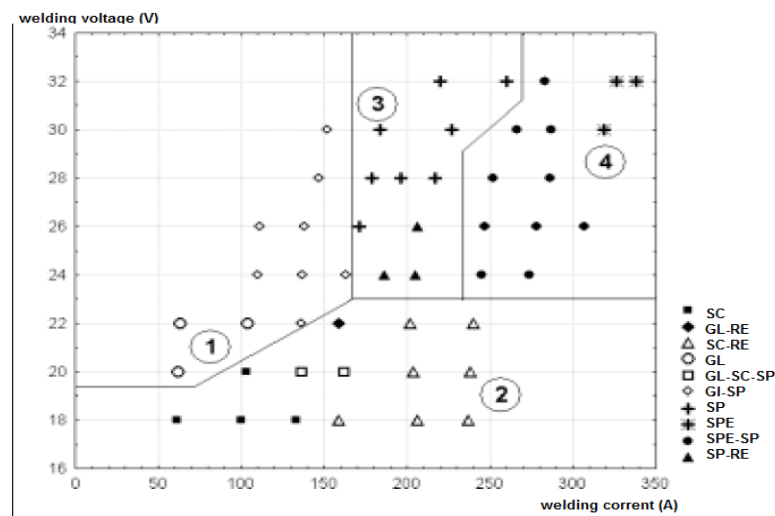


Figure 2.3.6: Metal transfer map for welding with shielding gas containing Ar+5% O₂ [3]

2.4 Vision System in Welding

If you had asked anyone in manufacturing some years ago, "What is your opinion of using a vision system in the welding environment?" you may have heard answers like "not practical," "too sensitive," "too costly," or "too much maintenance." But today's vision systems, with cameras placed before or after the welding operation, have robust enclosures designed for an industrial environment.

Currently, viewing systems are widely applied to aid studies of welding processes. The use of low- or high-speed cameras can provide different information that is useful to researchers, which is not possible to obtain with the usual monitoring of electrical signals such as current or voltage.

Despite the large current application, the idea of using a vision system is already disseminated from earlier times to digital photography. The first known work in this area [16, 4] was used a compound of an analog TV camera system and a TV monitor and projecting light through optical fibers to the application of a tracking system of the welding joint. Even at that time, was explored for the first time the idea of light in a specific spectrum ($0.63\mu\text{m}$) image acquisition with an interference filter ("bandpass") improving image contrast and decreasing light arc stemmed [17, 4].

Different viewing systems can provide specific information about the process in progress: the technique of backlighting (shadowgraph), i.e. projecting a shadow of elements in the weld area onto a flat surface as shown in Figure 2.4.1, permits visualization of drops in transfer as one way to study the metal transfer [18],

Whilst new viewing systems (figure 2.4.2) aim for direct visualization of the molten metal and the joint itself, with a range of applications ranging from study of the phenomena in the weld pool to joint tracking or online control of process parameters [4].

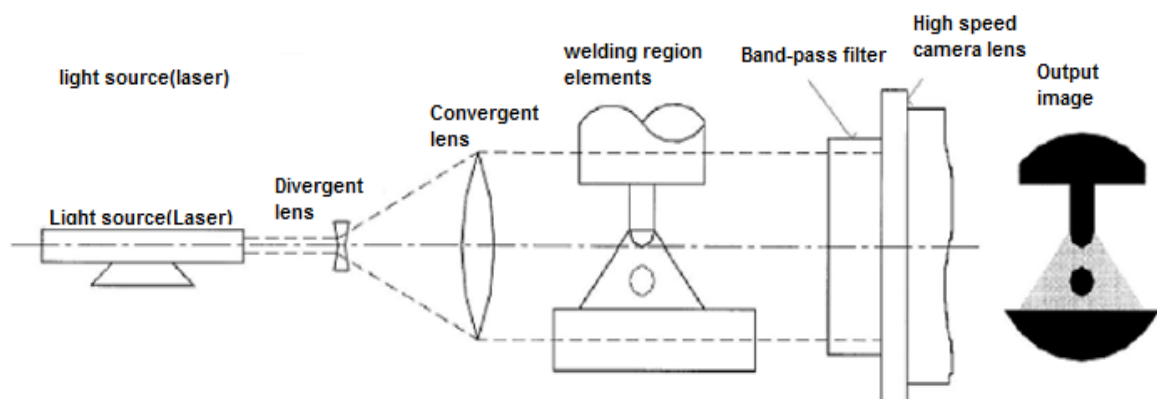


Figure 2.4.1: visualization of metal transfer by shadowgraph technique [18]

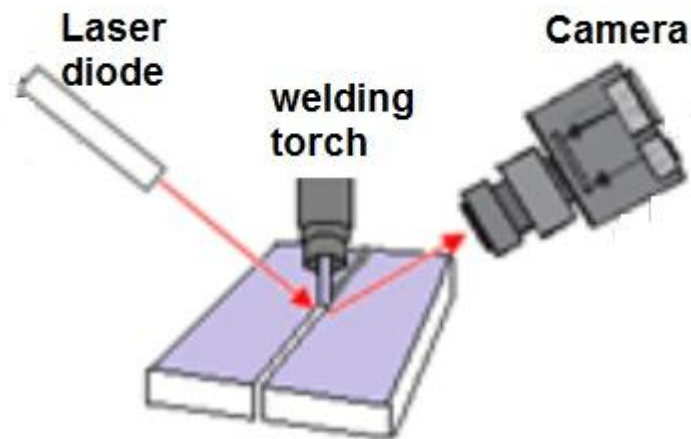


Figure 2.4.2: visualization of molten metal by indirect illumination [19]

Several studies were performed to obtain direct images of the weld pool, minimizing the light coming from the arc using interference filters ("bandpass") at different wavelengths. Some of the early work for direct viewing of the pool [20] used optical filters is around 950 nm for the study of the effect of protection and wire gas for MIG welding (Figure 2.4.3) and the study of the behavior of TIG welding puddle [4].

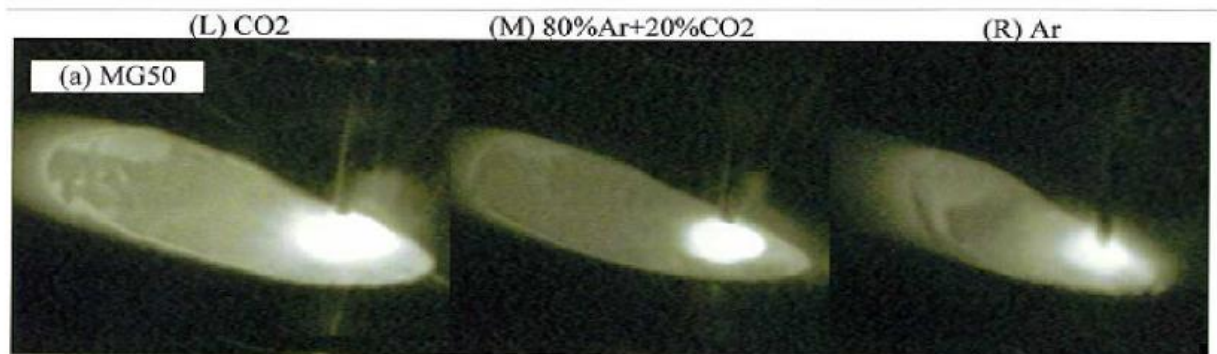


Figure 2.4.3: Images obtained with filter at 950 nm in the study of the MIG/MAG process [21]

Because the light radiation of the arc not be a problem during acquisition images, can also use the technique of Laser Illumination with Spectrum Filtering. The principle of the technique is to reduce or entirely eliminate the light from the arc that reaches the camera, illuminating the weld area with light from a laser [19]. In order to minimize the requirements of luminous intensity, the wavelength of the light from the light source should be selected where the intensity of the arc is low. A narrow band pass filter (interference filter) that is the same wavelength as the light source is necessary to reduce the light from the arc, and only laser light will be able to affect the camera, as shown in Figure 2.4.4 [4].

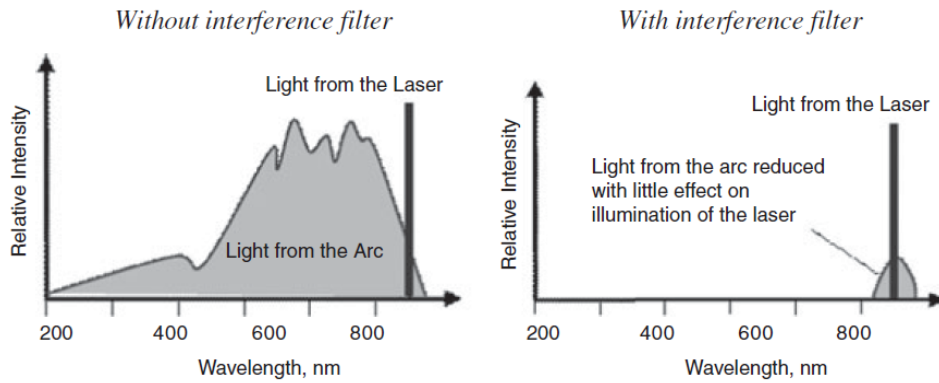


Figure 2.4.4: Principle of spectrum filtering [19]

The camera shutter time also influences the amount of light during acquisition of the image. Thus, it is possible to reduce the luminous intensity of the arc by decreasing the exposure time of each frame captured. Pulsing the laser within each exposure time makes it so that a minimum power is necessary for the laser light to overlap with radiation from the arc, as the laser pulse is within the exposure time of the camera per every frame acquired, as can be seen in Figure 2.4.5 [4].

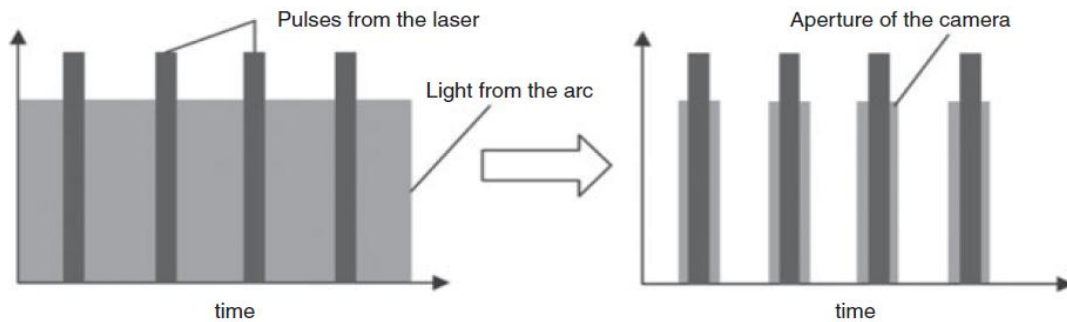


Figure 2.4.5: Set the exposure time of the camera to minimize the power applied to the pulsed laser compared to the continuous nature of the arc radiation [4]

According to Abdullah et.al [16] three different light sources can be used for illumination of the molten pool: laser systems, LED diodes and Laser diodes. Laser systems such as, e.g. the Nd-Yag laser, produces enough power to illuminate the molten pool, however are expensive and less flexible systems. The LED diodes are low-cost products and have a wide range commercially available, however, do not produce enough light output to illuminate molten pool. Since the laser diodes, have several characteristics that determine their usefulness as an alternative to the laser illumination itself, lower cost and having sufficient power when used together. It can be seen in Table 2.3.

Table 2.3: Characteristics of LED diodes and laser diodes [16]

Characteristic	LED Diodes	High-power Laser diodes
Current	50 to 100 mA	5 to 40 A
Potencial	Less than 1 W	50 W to 250 W
Opening Angle	Bigger than 40°	10° to 25°
Wavelength Available	0,66 to 1,65 μm	0,78 to 1,65 μm
Spectral Width	Large (40-190 nm FWHW)	Estreito (7-10 nm FWHM)
Cost	Less than £2	£15 to £400
Pulse Width	More than 100 μs	Less than 100 ns

Recent studies show the applicability of using high power laser diodes in the near infrared for vision systems of welding process. The light intensity emitted by the welding arc at infrared wavelengths above 850 nm is small compared to the visible spectrum. Figure 2.4.6 illustrates results obtained from this type of illumination technique [17, 4].

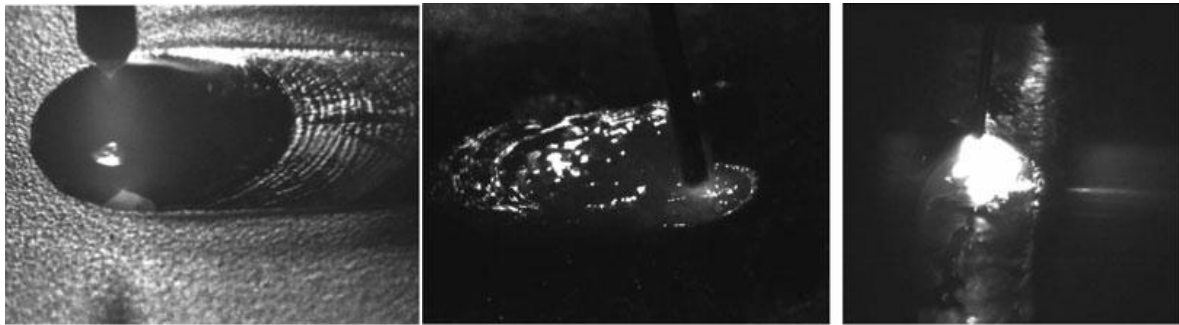


Figure 2.4.6: Viewing system with high-power laser diodes in near infrared for TIG (left) and MIG/MAG welding (center and right) [17, 4]

The choice of the NIR spectrum is mainly for two reasons. It is known that the emission of the light spectrum of the arc in welding processes covers the whole visible spectrum and emits at ultraviolet and infrared levels. However, emission in infrared has less light energy in comparison to the visible spectrum, facilitating the overlap of the arc in this region. On the other hand, to obtain a sequence of images illuminated by a beam of light in NIR is somewhat simpler and very low cost when compared with higher levels in infrared. A common complementary metal-oxide-semiconductor (CMOS) camera generally has response in the NIR spectrum, which would not be possible with the use of infrared light. A good example is the viewing of NIR LED by remote control TV with simple cameras. Infrared

cameras are product specific and therefore costly, yet ordinary cameras have a wide range of models at low prices and with high flexibility [22].

Knowing that the base component for the light source should be a high-power laser diode with emission in the NIR spectrum, and because there are few commercially available semiconductors for performing the classification, this study used the Osram model SPL PL90_3 pulsed laser diode, with the highest power available and greater applicability in this study. Table 1 lists the main characteristics of this laser diode, according to the manufacturer database.

It should be noted that the semiconductor selected is a pulsed laser diode; that is, the component supports only certain pulses of current passing through the joint at a certain time interval, and not the continuous flow of current. Specifically for this model, it is important to note that the laser diode has a very low duty cycle of 0.1%, maximum pulse width of 100 ns, and maximum peak current of 40 A [22].

Table 2.4: Characteristics of the SPL PL90_3 pulsed laser diode [22]

Parameters	Typical value	Unit
Work cycle	0.1	%
Emission wavelength	905	nm
Peak forward current	40	A
Beam divergence (FWHM)	11×25	°
Spectrum width (FWHM)	7	nm
Pulse width	100	ns
Peak power output	75	W

CHAPTER III

EXPRIMENTAL EQUIPMENT, MATERIALS AND METHODS

This chapter describes the equipment which used during the welding process, Also consumption of materials that used, are described with their respective specifications, equipment and accessories, as well as general assembly of experiments for conducting all tests needed. In addition, this chapter provides a description of the methodology that was used for completion of the proposed tests, as well as the selection parameters which aiming results quantitative and comparable.

3.1 Experimental Equipment

The main employed experimental equipment were:

- ✓ Welding power supply;
- ✓ Electrode wire feeding system;
- ✓ Welding torch;
- ✓ Coordinate welding table;
- ✓ Electrical data transient acquisition system (DAQ);
- ✓ Holding system for plates;
- ✓ Digital high speed camera and near-infrared vision system.

3.1.1 Welding power supply:

The power source provides electrical energy for the welding arc. For carrying out the welding tests, it used a multi process power supply. This welding power supply (IMC MTE Digitec 300) can be used for many processes such as SMAW, MIG/MAG, TIG and FCAW (Figure 3.1.1). It has a system of command with one keyboards and liquid crystal display, where the selection is made of processes and adjusting variables.



Figure 3.1.1: Welding power supply (IMC MTE Digitec 300)

Commercial arc welding power supplies are typically classified to operate in one of two modes: constant current or constant voltage. The power sources generally recommended for flux-cored arc welding are direct current constant voltage type. Direct current can be either reverse or straight polarity. Flux-cored electrode wires are designed to operate on either DCEP or DCEN. The wires with an external gas shielding system are generally designed for use with DCEP. Some self-shielding flux-cored ties are used with DCEP while others are developed for use with DCEN. Electrode positive current gives better penetration into the weld joint. Electrode negative current gives lighter penetration and it is used for welding thinner metal or metals where there is poor fit-up.

Finally, for the tests, the power source was adjusted to work with MIG/MAG Conventional and operating in the constant voltage mode and direct current reverse polarity (DC+).

3.1.2 Electrode wire feeding system:

The wire feed speed regulates how much or how fast the wire is feed into the weld joint that measured in inches per minute (in/min - IPM) or meters per minute (m/min). Welding current (measured in amps) and resulting penetration levels are directly related to wire feed speed rates. A wire feed motor provides power for driving the electrode through the cable and gun to the work.

There is several different wire feeding systems available. In this case, it was used; the wire feeder "IMC STA-20" which it has electrode wire feed speed between 2.0 to 20.0 m/min (calibration equation: $WFS_{real}=1.0274 WFS_{adjust}$) and also admits electrode wire diameters in the range 0.60 to 1.60 mm (Figure 3.1.2).



Figure 3.1.2: Electrode wire feeding system (IMC STA-20)

One of some different between the MIG/MAG process and Tubular electrode process is the type of rollers. As illustrated by Figure 3.1.3, during FCAW welding, it is used knurled V- or U-groove drive rolls in the wire feeder. Compared to a GMAW solid welding wire (which uses a smooth V-groove drive roll), FCAW wire is much softer (due to its tubular design) and if it utilized the incorrect drive roll, it can easily compress the wire. Cored electrodes also require the use of knurled drive rolls. A cored electrode cannot withstand as much drive roll tension or squeezing force as a solid electrode can with smooth drive rolls. The electrode would be crushed or deformed. The drive roll's knurls (i.e. teeth) help grip the cored electrode, providing equivalent pushing force, but with less drive roll tension.

Also know that should be set the tension of the rollers before starting the machine. The tension should be just enough to feed the wire without slipping. Setting the correct drive roll tension can prevent the wire from flattening and becoming tangled. To set the proper

tension, begin by releasing the tension on the drive rolls. Increase the tension while feeding the wire into the palm of your welding glove and continue to increase the tension one half turn past wire slippage. If you tighten up the rollers too much, the wire will get crushed and then you will need to refeed the wire.

A wire feeder consists of an electrical motor connected to a gear box containing drive rolls. Inside the wire feed section of each GMAW or FCAW machine there will be a 2 drives or 4 drives roller set up. The four rollers set up provide a more constant feed capable of pushing the wire over a further distance.

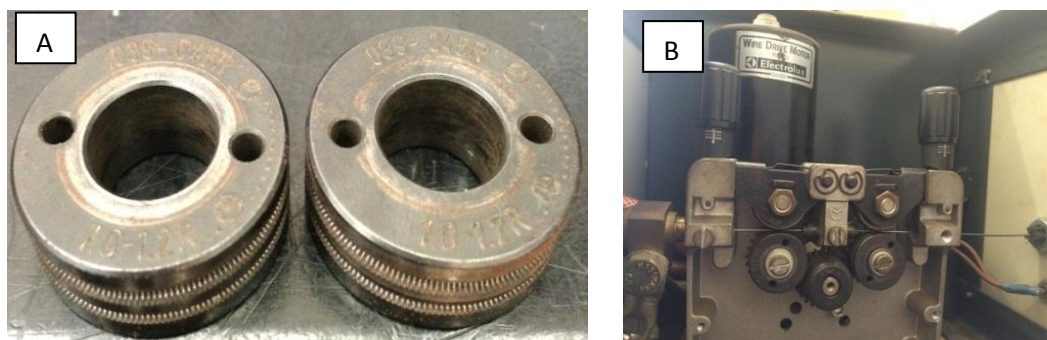


Figure 3.1.3: A) Knurled V groove rolls for FCAW B) The 4 rollers set up wire feeder

3.1.3 Welding torch:

A welding torch is used in an automatic welding system to direct the welding electrode into the arc, to conduct welding power to the electrode, and to provide shielding of the arc area. There are many types of welding torches, and the choice depends on the welding process, the welding process variation, welding current, electrode size and shielding medium.

Welding torches can be categorized according to the way in which they are cooled. They may be water-cooled with circulating cooling water or air-cooled with ambient air. A torch can be used for a consumable electrode welding process such as gas metal arc or flux cored arc welding, and shielding gas may or may not be employed.

The major function of the torch is to deliver the welding current to the electrode. For consumable electrode process this means transferring the current to the electrode as the electrode moves through the torch.

A second major task of the torch is to deliver the shielding gas, if one is used, to the arc area. Gas metal arc welding uses a shielding gas that may be an active gas usually carbon dioxide or a mixture of an inert gas, normally argon, with CO₂ or oxygen.

In this work it was used an automatic straight torch with current capacity up to 400 A, with an approximate length of 2 meters, water cooled and equipped with a steel contact tip for the wire with 1.2 mm diameter and shielding nozzle (Figure 3.1.4).



Figure 3.1.4: Welding torch, steel contact tip and shielding nozzle

3.1.4 Coordinate welding table:

All the applications are involved in automated positioning are for time saving and reducing human error. The welding table is one of these systems for displacement and positioning. In this case the equipment allows you to control the table movement in the X axis and the torch on the Y axis, although in this work, the control is only for orientation of the table, according to a single axis, the X and with the welding travel speed (displacement in x-axis) up to 45 cm/min (Figure 3.1.5).



Figure 3.1.5: Welding table

3.1.5 Electrical data transient Acquisition system (DAQ):

Data acquisition is the process of sampling signals that measure real world physical conditions and converting the resulting samples into digital numeric values that can be manipulated by a computer. Data acquisition systems (abbreviated with the acronym DAQ) typically convert analog waveforms into digital values for processing [23].

The acquisition of the current signals and welding voltage was performed by a system data acquisition installed on a microcomputer with rates of 5 kHz, and an 8-bit resolution. In addition, in this case for acquisition of welding current signals, the system uses a Hall sensor, brand LEM SA and model LT 500-T, with measuring range of 0 to 500 A and to monitoring of the voltage, the system uses a divisor of voltage with a measurement range from 0 to 60 V (Figure 3.1.6).

After installing the DAQ system for measuring, can use the LabVIEW programming software to visualize and analyze data as needed (Figure 3.1.6D). LabVIEW is a graphical development environment by National Instruments for creating flexible and scalable test, measurement and control applications rapidly and at minimal cost. With LabVIEW, engineers and scientists interface with real-world signals, analyze data for meaningful information and share results and applications. Regardless of experience, LabVIEW makes development fast and easy for all users [24].

After all process of measuring with DAQ system and LabVIEW, it was used "OriginPro 9.0" (Figure 3.1.6E) to crate the graphics which need in this study. This software was used to calculated mean/average values. For example, the mean voltage or voltage average can be calculated mathematically by Equation 3.1. In addition, the effective value or RMS (Root mean square) can be mathematically calculated for voltage by the Equation 3.2. These calculations were also employed for welding current.

$$U_m = \frac{1}{N} \sum_{i=1}^N U_i = \frac{U_1 + U_2 + \dots + U_N}{N} \quad \text{Equation 3-1}$$

$$U_{rms} = \sqrt{\frac{1}{N} \sum_{i=1}^N U_i^2} = \sqrt{\frac{U_1^2 + U_2^2 + \dots + U_N^2}{N}} \quad \text{Equation 3-2}$$

Where:

- U1, U2 - measured instantaneous values of Voltage;
- N - Number of measurements at regular intervals.

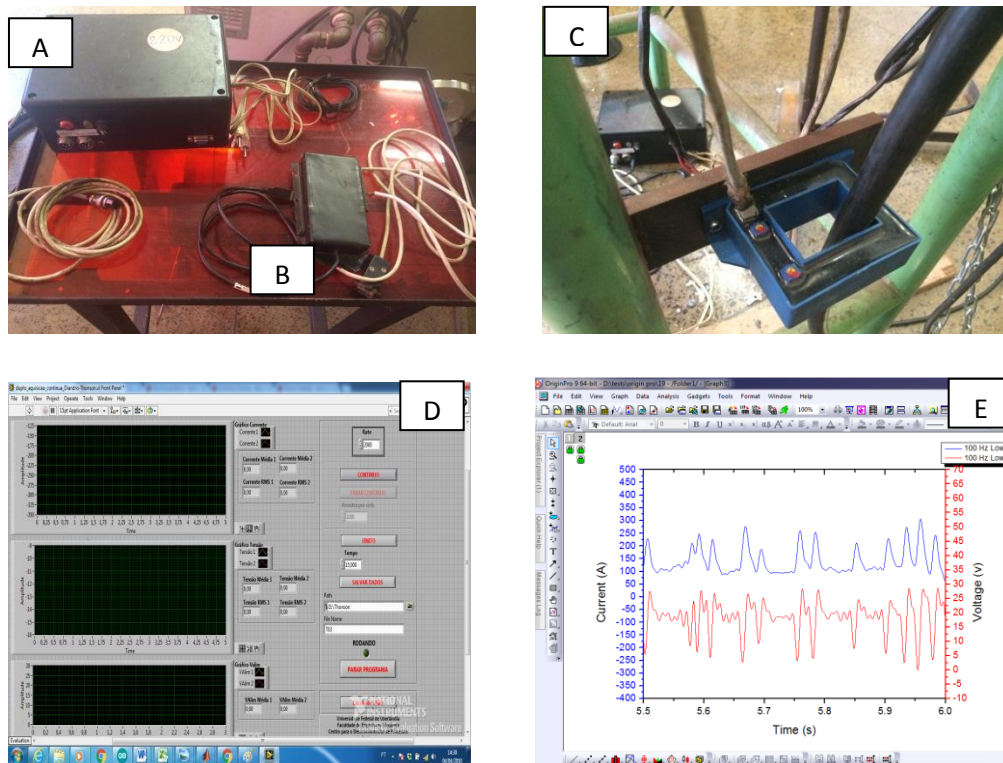


Figure 3.1.6: A) Signal Conditioner; B) Acquisition board; C) Hall Effect sensor; D) LabVIEW programming software; E) OriginPro 9.0 application.

3.1.6 Holding system for plates:

During the welding operation, are required specialized fixtures to accurately hold the work piece and prevent deformation during welding, due to the high heat density involved with the processes in welding, Thus, in this case it used a clamp which is illustrated in Figure 3.1.7.

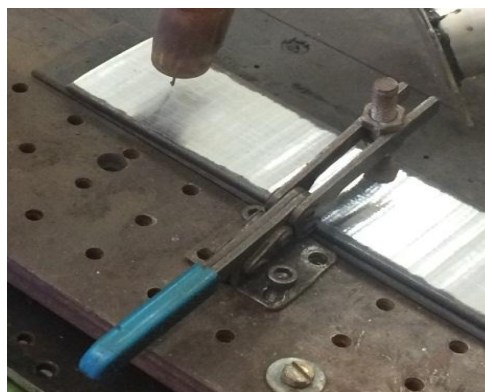


Figure 3.1.7: Clamping system for supporting of plate during the welding process.

3.1.7 Digital High Speed Camera and Near-infrared vision system:

The welding process has two inherent obstacles for viewing by traditional methods. First, it is extremely bright, which causes conventional cameras to “flare out,” and second, the process occurs very quickly making it too quick for standard cameras to record in any valuable detail , it means that the moving speed of target in observing area is quite high.

In addressing the first of these issues, in this paper is utilized near infrared (IR) laser illumination device which called ViaSolda [4] and an optical interference filter at 905nm that blocks out all wavelengths of light other than IR. This gives illumination to the image even with no welding flare and permits the user to effectively see through the glare to view the process that is occurring. The IR laser also provides live illumination to the surrounding environment making setup of the camera focus simple. Note that with ViaSolda, images from 30 up to 300 frames per second are possible to be obtained.



Figure 3.1.8: Source of Infrared (ViaSolda)

With regard to the second obstacle to viewing the welding process, the fact that it occurs too quickly for conventional cameras to capture in any meaningful detail, high speed video is expressly designed for this purpose. This is the main reason why high-speed video technique is necessary for visual analysis of welding processes for viewing both droplet formation and weld pool activity in good detail.

Standard cameras record at either 25 or 30 frames or picture per second. If an object is moving extremely fast, the camera may miss it as it moves or it may just appear as a blur as it continues to move during the camera exposure. High-speed video cameras capture images at higher speeds. Typically, speeds of around 2000 fps and a shutter speed of around 5 μ s are required to capture high-resolution images.

With the help of high speed camera equipment, researchers can now directly observe melt flow phenomena which only could be imagined or simulated in the past. In this paper for filming at high speed, it used the camera HiSpec 5 which is available in the laboratory. Also because only the emission spectrum of the near infrared laser diodes should be able to reach the camera, utilized an optical filter interference at 905 nm with specification Edmund Optics Filter BP 905nm X 25MM 10NM OD4 (Figure 3.1.9).



Figure 3.1.9: High speed digital camera (HiSpec 5) and filter

Its compatibility with the prototype ViaSolda it was validated through experimental tests, to obtain images of the motion of the molten metal inside the keyhole at 300 fps to provide information and analyze the metal transfer of FCAW process.

The camera setup is done entirely through HiSpec Control Software. After connected to the software the following settings should be modified for use with the ViaSolda prototype: framerate (300 fps), shutter (2 μ s) and enable sync in, as illustrated in Figure 3.1.10.

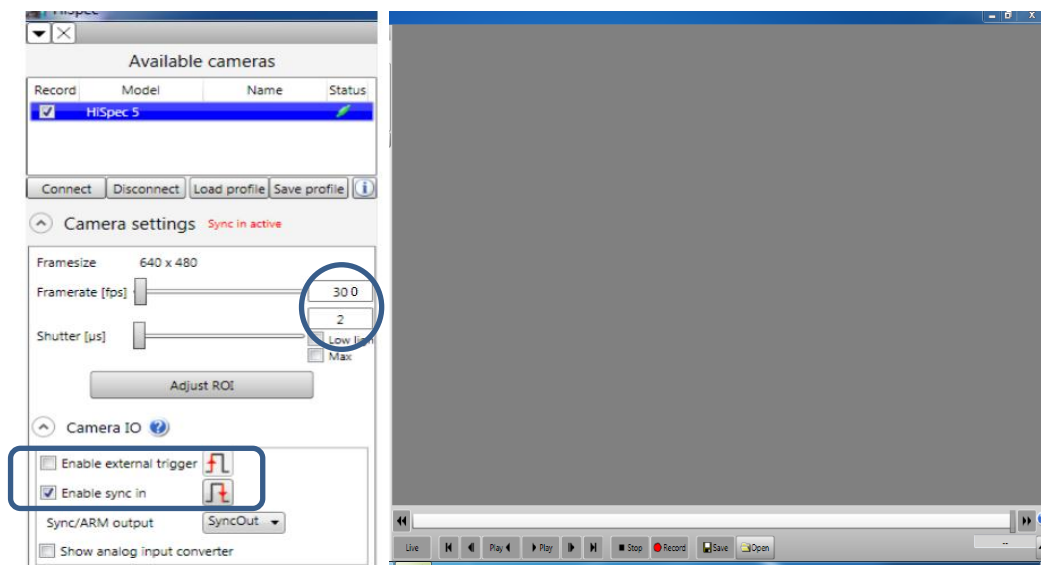


Figure 3.1.10: HiSpec 5 home Screen Software

3.2 Material and Consumable

In this item are listed and detailed, material and consumables, which were used for the tests such as shielding gas, electrodes and metal base.

3.2.1 The shielding gas:

There are two fundamentally different types of flux-cored welding process. One type is self-shielded and the other type is gas-shielded. These two types are often subcategorized as the SS-FCAW process (self-shielded, flux-cored) and GS-FCAW process (gas-shielded, flux-cored) which explained more complete in the part of literature review.

The difference in the two is due to different fluxing agents in the consumables, which provide different benefits to the user. Usually, self-shielded FCAW is used in outdoor conditions where wind would blow away a shielding gas. The fluxing agents in self shielded FCAW are designed to not only deoxidize the weld pool but also to allow for shielding of the weld pool and metal droplets from the atmosphere.

The flux in gas-shielded FCAW provides for deoxidation of the weld pool and, to a smaller degree than in self-shielded FCAW, provides secondary shielding from the atmosphere. The flux is designed to support the weld pool for out-of position welds. This variation of the process is used for increasing productivity of out-of-position welds and for deeper penetration.

Gas-shielded, flux-cored arc welding (GS-FCAW) is a very popular and versatile welding process. It is used with mild steel, low-alloy steel and other alloy materials in a variety of applications, such as heavy fabrication, structural, shipbuilding and offshore. The two most common (but not exclusive) shielding gases used with the GS-FCAW process are carbon dioxide (CO_2) and a binary blend of 75% argon (Ar) / 25% CO_2 . Other blends, such as 80% Ar / 20% CO_2 , can also be used [25]. A high percentage of argon gas in the mixture tends to promote higher deposition efficiency due to the creation of fewer spatters.

Shielding gas equipment used for gas shielded flux-cored wires consists of a gas supply hose, a gas regulator, control valves, and supply hose to the welding gun. In this case, it was used 75% Ar and 25% CO_2 , as a shielding gas. Also gas flow rate in this work is 14 l/min, which was regulated by the pressure regulator and checked by a flowmeter.

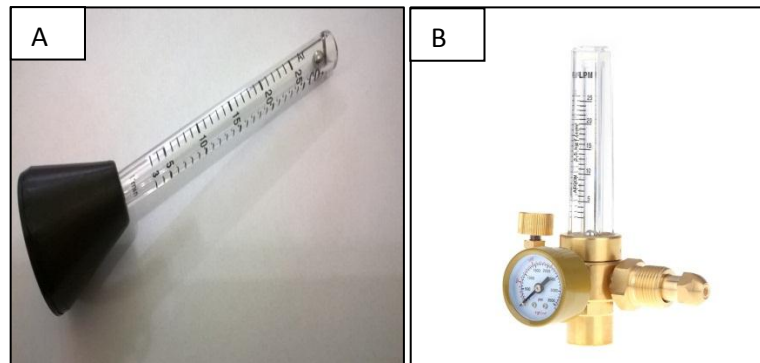


Figure 3.2.1: A) Flowmeter, B) regulator

3.2.2 Filler metal or electrode:

There are many types of materials used to produce welds. These welding materials are generally categorized under the term filler metals, defined as "the metal to be added in making a welded, brazed, or soldered joint. The filler metals are used or consumed and become a part of the finished weld. The definition has been expanded and now includes electrodes normally considered non-consumable such as tungsten and carbon electrodes, fluxes for brazing, submerged arc welding, electro slag welding, etc. The term filler metal does not include electrodes used for resistance welding, nor does it include the studs involved in stud welding [26].

As a general discussion of flux-cored welding, The American Welding Society (AWS) classifies all tubular electrodes having a flux on the inside as "flux-cored" wires, and calls it the Flux Cored Arc Welding (FCAW) process. All flux-cored wires have some similar characteristics. These include forming a protective slag over the weld, use a drag angle technique, have the ability to weld out-of-position or flat and horizontal only at higher deposition rates (depending on type of wire), ability to handle contaminants on the plate, etc [25].

Classification for FCAW wire is designed to tell the user the ultimate tensile strength of the as welded weld metal, the position(s) it can be used in, and its usability characteristics.

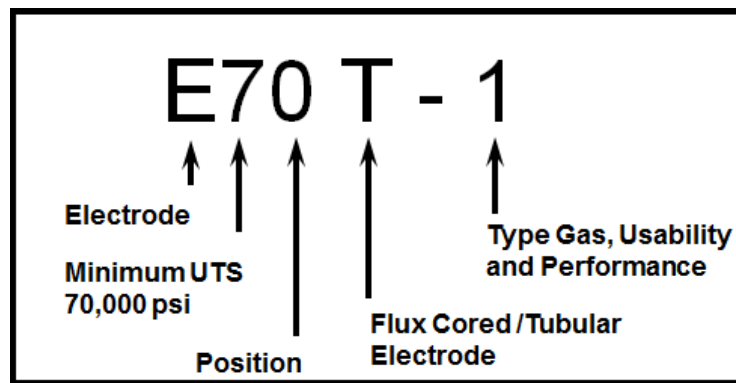


Figure 3.2.2: FCAW Electrode Classification (AWS Specification- A5.20)

In the example above, the ultimate tensile strength of the weld metal is specified as 70 ksi. Positions the electrode can be used in are specified by the third item in the specification, 0- for flat and 1 for all positions. The “T” designates that this is a flux cored wire. The usability and performance of the consumable is specified after the dash. In the example above the 1 stands for a general purpose electrode using DCEP and for multi-pass welding. In this work it used E71T-1 (Lincoln Electric) with 1.2 mm diameter.

For semi-automatic out-of-position welding, E71T-1 wires offer unsurpassed performance. Its fast freezing rutile slag provides the highest deposition rates in the vertical-up position, up to 7 pounds per hour, unmatched by any other semi-automatic arc welding process. In addition, the E71T-1 wires also offer an exceptionally smooth welding arc and minimal spatter, even with 100% carbon dioxide shielding gas. Argon/carbon dioxide blends are used for the smoothest arc and best out-of-position performance. These are reasons why E71T-1 is the world's most popular flux-cored wire. It is a top choice for shipbuilding, structural steel, and general steel fabrication applications [27].

3.2.3 Metal base and workpiece:

The base material which was selected for the preparation of tests in this study was AISI ABNT 1020 low carbon steel, as shown the chemical composition in Table 3.1. Also to finding the dimension and preparing of workpieces, it utilized Rosenthal and Adams equation with some machining equipment, which explained in two below steps.

Table 3.1: Nominal chemical composition of AISI 1020 steel

Element	Content
Carbon, C	0.17 - 0.230 %
Iron, Fe	99.08 - 99.53 %
Manganese, Mn	0.30 - 0.60 %
Phosphorous, P	≤ 0.040 %
Sulfur, S	≤ 0.050 %

A) Dimension of test plates

Usually, in the welding tests using a very large plate size, which is not necessary, due to the cost overruns, is not recommended. Also in these tests, due to the filming of weld pool, use a plate with very small dimensions, due to the rapid melting and inability to capture the molten pool, is not recommended. So the shape of workpiece calculated for an infinite plate by length, width and thickness. Thus it needs to specify boundary conditions for the workpiece. There are some equation such as Rosenthal's and Adams' ones, which can provide only an approximate presentation the temperature distribution in a weld. These solutions get a general idea of the characteristics of heat flow in welding for many cases of interest.

The American Welding Society recommends that,

If $\tau > 0.9$, the plate is considered thick

If $\tau < 0.6$, the plate is considered thin

If $0.6 < \tau < 0.9$, is a transition zone that can result in errors.

The relative thickness (τ), a dimensionless parameter, is calculated by Rosenthal equation, where:

$$\tau = \frac{h}{h_{crit}} = h \sqrt{\frac{\rho c (T_e - T_0)}{H_L}} \quad \text{Equation 3-3}$$

- h = plate thickness (mm) that to be evaluated;
- h_{crit} = The critical thickness (mm) , which distinguishes between the cooling conditions of thin and thick plate;
- ρ = density of the base material (g/cm³);
- c = specific heat of the base material (J/g °C);

- T_e = expected temperature that to be reached by the material in opposite face of bead ($^{\circ}\text{C}$);
- T_0 = initial temperature (or preheating) ($^{\circ}\text{C}$);
- H_L = heat input (kJ/mm);

Heat input (H_L) is given by Equations 3-4, where:

$$H_L = \eta H = \eta \frac{VI.60}{v.1000} \quad \text{Equation 3-4}$$

- η = thermal efficiency;
- H = welding energy (kJ/mm);
- v = welding speed (mm/min);
- V = Welding voltage (V);
- I = welding current (A).

In this study, it considered below value of parameters to find approximate thickness of a thin plate (h).

Table 3.2: Welding parameters to find plate thickness

$T < 0.6$	ρ	c	T_e	T_0	η	v	V	I
0.5	7.85	0.63	1200	22	0.8	45	36	400
-	g/cm^3	$\text{J/g } ^{\circ}\text{C}$	$^{\circ}\text{C}$	$^{\circ}\text{C}$	-	cm/min	V	A

To calculate of plate width, for a thin plate ($T < 0.6$), utilized Adams equation for Peak Temperatures. The dimension (Y), distance from the center of weld bead to the desired contour is given by Equation 3-5 where:

$$Y = \frac{\frac{1}{(T_p - T_0)} - \frac{1}{(T_f - T_0)}}{4.13 \rho h \frac{c}{H_L}} \quad \text{Equation 3-5}$$

T_p is the maximum or peak temperature of the edge of the test plate, which utilized 300°C in this study and T_f is the melting temperature of the base material, which is 1540°C for carbon steel plate.

Finally the plate thickness that was calculated by Equation 3-3 and the plate width which calculate by Equation 3-5 are equal to $h=0.8$ cm and $2Y=5.4$ cm which were only an approximate presentation for dimensions. Also according to situation of welding table and holding system considered 200 mm for length of workpieces. As a result, it utilized a square mil steel with 5mm thick x 50mm width x 200mm long, which was available in the laboratory and more similar to dimensions of calculated plate.

B) Workpiece Preparation

Before starting a weld, the plate edges should be carefully cut and prepared. The bandsaw machine is a machine tool designed to cut material to a desired length or contour. It functions by drawing a blade containing cutting teeth through the workpiece. The sawing machine is faster and easier than hand sawing and is used principally to produce an accurate square cut on the workpiece. Metal cutting bandsaw machines fall into two basic categories: horizontal machines and vertical machines. In this work study as a first, utilized a horizontal bandsaw machine (Figure 3.2.3A), which was available in laboratory to cut the steel workpiece.

Albedo or reflection coefficient is the ratio of reflected radiation from the surface to incident radiation upon it. Its dimensionless nature lets it be expressed as a percentage and is measured on a scale from zero for no reflection of a perfectly black surface to 1 for perfect reflection of a white surface. So after cutting the workpiece with true dimension utilized a surface grinder machine (Figure 3.2.3B) to cleaning the metal and remove all surface mill scale and rust to have a white surface and lower roughness for maximum reflection of light from source of infrared (ViaSolda) to surface of workpiece and after that to high speed camera (HiSpec5).

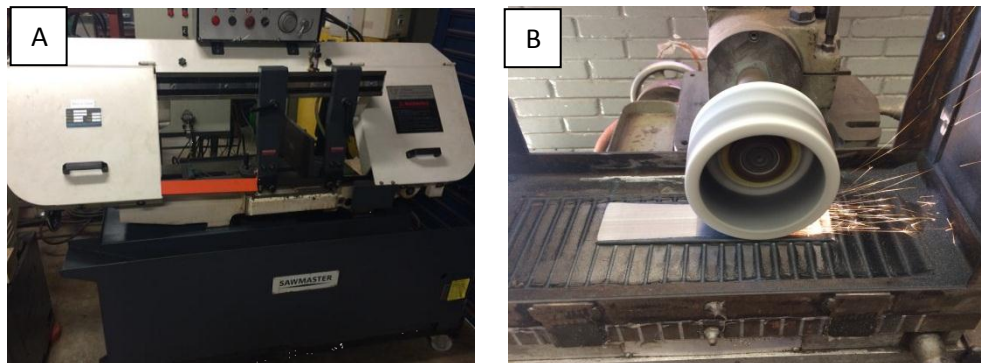


Figure 3.2.3: A) horizontal bandsaw machine B) surface grinder machine

3.3 Methodology

Thus, from a methodological point of view, to achieve the objective of this study, different welding parameters were utilized and experiments were planned which are explained in below.

3.3.1 Contact Tip to Work Distance (CTWD)

CTWD (contact tip to work distance) is, the distance from the end of the contact tip to the plate or work piece. ESO (electrical stickout, or more technically correct, electrical extension), is the distance from the end of the contact tip to the top of the welding arc. The difference between the two is the height of the arc.

$$\text{ESO} = \text{CTWD} - \text{Arc Length} \quad \text{Equation 3-6}$$

In this study, utilized 18 mm for CTWD and also as in free flight metal transfer types needs bigger CTWD or bigger arc length than short circuit metal transfer type so in this case witch used both metal transfer type for tests, the distance between nozzle and contact tip is equal of zero (figure 3.1.1B).

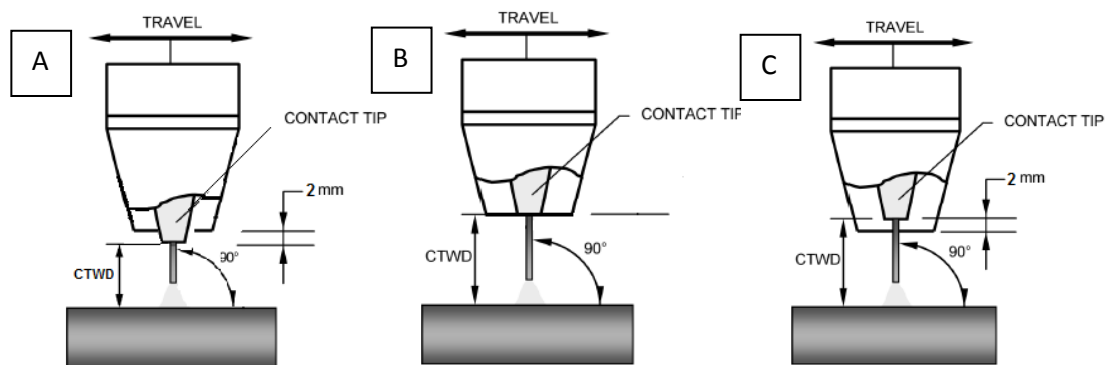


Figure 3.3.1: A diagram showing the contact tip position relative to the shielding nozzle used during welding

3.3.2 Torch Angles

The angles at which you hold the electrode and torch are important to weld quality. These include the travel angle and work angle, both measured in degrees. Travel angle is the angle between the electrode and a line perpendicular to the surface of work piece, as

measured from the weld side view. Forehand, perpendicular, and backhand are the terms most often used to describe the gun angle as it relates to the work and the direction of travel. The forehand technique is sometimes referred to as pushing the weld bead, and backhand may be referred to as pulling or dragging the weld bead. The term perpendicular is used when the gun angle is at approximately 90° to the work surface. Pushing can cause the arc to ride on top of puddle instead of in front of it, resulting in less penetration and is on the contrary, in pulling. In Perpendicular technique, the weld's penetration and reinforcement are balanced between those of forehand and backhand techniques (figure 3.3.2).

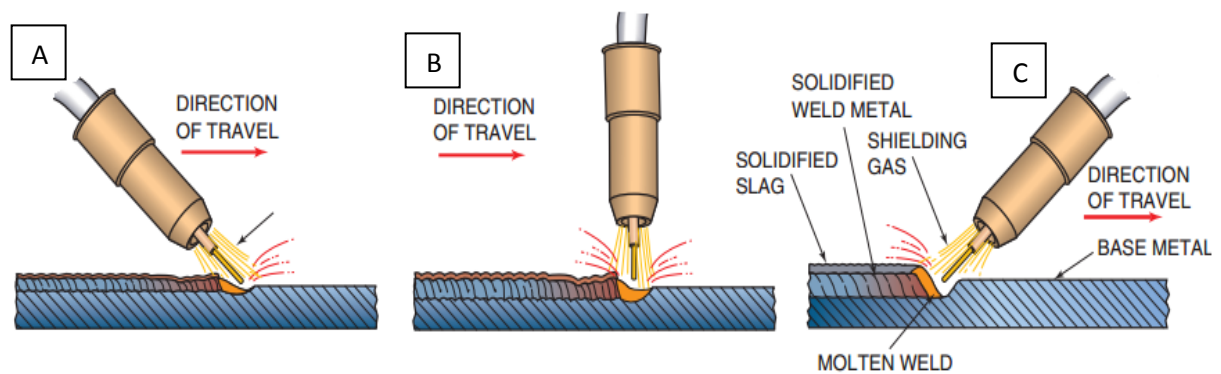


Figure 3.3.2: Travel angle. A) Forehand, B) Perpendicular, and C) Backhand angles [4]

Work angle is the angle between the electrode and surface of work piece, as measured from the weld end view. For a butt joint, typically use a 90° work angle and for a corner, tee or lap joint, typically use a 40° to 45° work angle (figure 3.3.3). The travel angle and work angle which utilized in this work is equal to 90° .

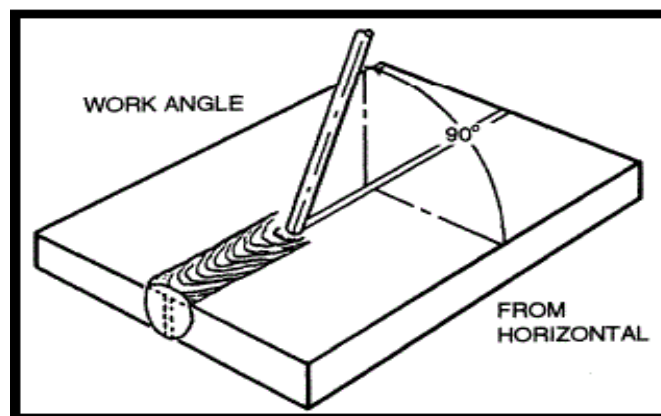


Figure 3.3.3: work angle [27]

3.3.3 Voltage, Wire Feed Speed and Travel speed,

As the some literature review study about monitoring of metal transfer for FCWA process, in this work decided to utilize 18 V up to 40 V as a voltage and 4 m/min up to 20 m/min as a wire feed speed. Also as explained in Section 3.1.4 (Coordinate welding table), welding travel speed is up to 45 cm/min.

Therefore, with the above-mentioned values of wire feed speed and voltage, created the experimental design with the special number for each test as illustrated in Table 3.3.

Table 3.3: Experimental design showing the test numbering (from 1 to 108)

U(v)											
40		100	101	102	103	104	105	106	107	108	
38		91	92	93	94	95	96	97	98	99	
36		82	83	84	85	86	87	88	89	90	
34		73	74	75	76	77	78	79	80	81	
32		64	65	66	67	68	69	70	71	72	
30		55	56	57	58	59	60	61	62	63	
28		46	47	48	49	50	51	52	53	54	
26		37	38	39	40	41	42	43	44	45	
24		28	29	30	31	32	33	34	35	36	
22		19	20	21	22	23	24	25	26	27	
20		10	11	12	13	14	15	16	17	18	
18		1	2	3	4	5	6	7	8	9	
		4	6	8	10	12	14	16	18	20	WFS(m/min)

To carrying out the welding tests, it was kept a deposition constant, that is, a relationship between the electrode wire feed rate and welding speed. It was done with the aim of maintaining a constant reference between tests. Thus, to calculate of welding travel speed for each test, utilized a constant value, which achieved by, divided of the maximum wire feed speed to the maximum welding travel speed, as in Equation 3.7.

$$\text{Max WFS} / \text{Max Ws} = 20/45 = 0.44$$

Equation 3-7

Finally, it was utilized 0.44 as a constant value to calculate welding travel speed. In Equations 3.8 and 3.9, there is some example to use the table and calculate of welding travel speed:

Test number 49:

$$U= 28 \text{ V, WFS}=10, W_s=(10/0.44)=22.72$$

Equation 3-8

Test number 80:

$$U= 34 \text{ V, WFS}=18, W_s=(18/0.44)=40.90$$

Equation 3-9

3.3.4 Position of systems form interest area

Achieving the images of metal transfer to show perfectly the electrode, arc length, droplets and melting pool is the great practical importance in this study. The distance and angle of systems from the plate are two important parameters of positioning to achieving the good-quality images of metal transfer.

The facility includes a telescopic arm to assist the positioning of the prototype (ViaSolda) and a tripod for the positioning of the high-speed camera. The shorter distance between the light-emitting device and the receiver, the brighter images can be achieved. So is better to utilized minimum safety distance between ViaSolda and the plate. But on the other side, when utilized minimum safety distance, because of the different arc length in different metal transfer type, sometimes couldn't see the electrode on the screen of monitoring software (because it is very near). Because of that, the system was positioned with different distance from the area of interest. Test number 100 which has maximum Voltage and minimum wire feed speed (lowest arc length) is the best for adjusting of these distances. The minimum distance allowed was 100 mm between the plate to prototype of ViaSolda and 190 mm from plate to the high-speed camera. The lighting is projected onto the surface of the plate at an angle rate between 22.5° up to 25° and the camera positioned with a symmetrical angle in relation to the plane of the plate to receive the maximum reflection of light from the laser diodes. Also in this study utilized the 3-dimensional imagery technic for the positions of systems to have a better visualization of the weld pol, weld bead and metal transfer as illustrated in Figure 3.3.4. All these positions are fixed, up to finish all the tests.

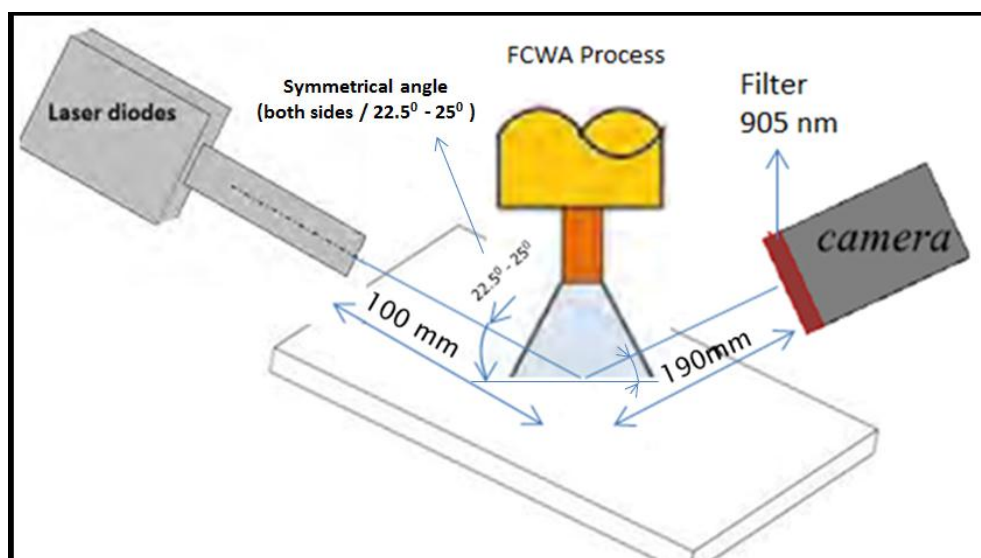


Figure 3.3.4: Schematic of 3-dimensional imagery technic positioning

3.3.5 Measurement of the arc length

There is a difficulty in experimental studies published regarding the definition and measurement of the arc length which making this subjective measurement that is dependent upon the criteria used by each author. In these particular tests, in some pictures arc light reflexes to the other part of weld bead (Figure 3.3.5 A). Thus, the measurement can be with error if used the arc light to measure the arc length. Also in some picture cannot find exactly the arc light for measuring of the arc length (Figure 3.3.5 B). Because of these problems, it was used a reference point for all photos which is the point that electrode will start to melt and changes it color up to surface of molten pool (Figure 3.3.5 C,D).

For measuring of arc length it was utilized “ImageJ”, as a software and electrode diameter, as a reference distance for each photo. To carry out the measures of the arc length, 40 consecutive frames was used, also the mean value of arc length and standard deviation calculated by these 40 photos. But sometimes, the electrode was on the weld pool and in these photos (Figure 3.3.5 E) cannot measure exactly the arc length, but cause the movement of weld pool in other photos can measured the arch length (Figure 3.3.5 F). Thus, to solve this problem, the complete cycle (set) of images was deleted and another cycle to this group of photos was added to have a true mean value. Also, in free flight type with the metal transfer buried inside the weld pool (this situation will be further explained in Chapter IV), there is not any short circuit at any cycle of metal transfer, thus the set is not necessary to be consecutive. Therefore, it was employed 40 photos of all, which, because of the movement of weld pool can see the arc length and is possible to measure it.

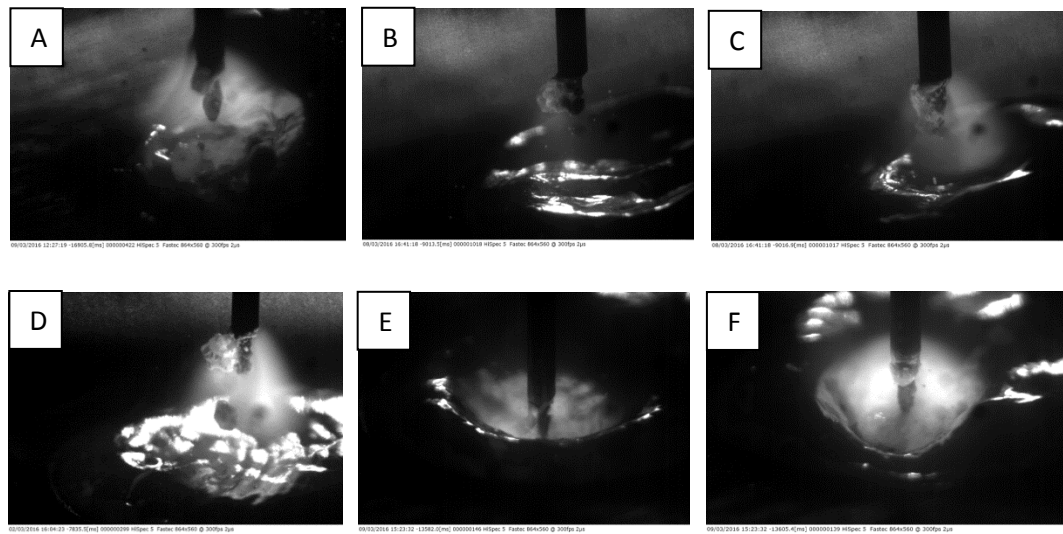


Figure 3.3.5: Observation of different arc lengths

Finally as a schematic view to measuring of arc length, can explained the different type of measuring for each situation. When the electrode is completely on the weld pool and it have contact with weld bead so the arc length can be zero (Figure 3.3.6 a). This happened in most of images of short circuit transfer. If the electrode just has contact with surface of weld bead the arc length can be the distance that electrode will start to melt up to surface of weld bead (Figure 3.3.6 b). This type of measuring happened in most of transition area when there are short circuit and free-flight transfers together. Actually in this situation, the electrode is very near of weld bead surface and sometime has contact with it (short circuit) and sometimes has not (free flight).

Thus, with this approach of measuring technique, it is possible to observe the position of the electrode tip that is far from surface, but sometimes short circuits happens because the growing of the droplet diameter. In other scenario, when there are no contact between the electrode and weld bead, the measurement of arc length can be carried out as show in Figure 3.3.6 c. If the electrode is on the weld pool, the arc length can be measured just when the weld pool moves and the arc length can be seen, as illustrated in Figure 3.3.6 d.

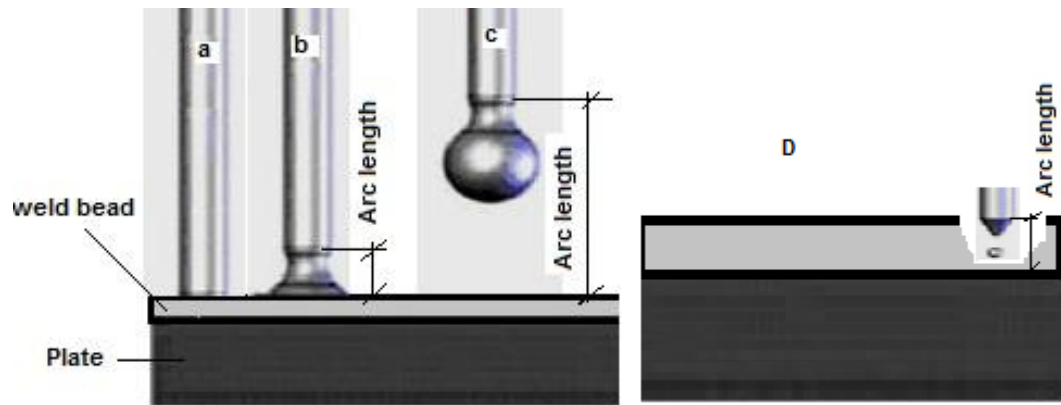


Figure 3.3.6: Schematic view to measuring of arc length in different situation

3.3.6 Turning on the ViaSolda

According to Mota [28], when turn on the ViaSolda, laser diodes started to be hot. Because of this, the intensity of infrared laser is reduced by more time and the quality of images is reduced too. Since in this study is important to have photos of the stable part of welding, so it decided to turn on the ViaSolda after some primary second of welding.

3.3.7 Drawing the metal transfer maps

With the calculated mean values and the reference values for current, welding voltage, arc length and welding speed, Excel software was used to draw the maps with the metal transfer modes that are presented on Chapter IV (results and discussion).

3.3.8 Preparation of welding environment

Arc welding not only produces a brilliant light, but it also emits ultraviolet and infrared rays that are very dangerous for eyes and skin. Especially in this study which it utilized near infrared laser. Personal safety items include helmets, lenses, and gloves. An important item that needs to be covered here is welding screens. The welder not only has to protect himself but also must take precautions to protect other people who may be working close by. When doing welding in the field/shop, it must be installing a welding screen around the work area. It can be an elaborate factory-manufactured screen or as simple as one constructed on site from heavy fire-resistant canvas. In this study utilized transparent welding curtains to interlock and enclose a work area to protect other people and also utilized a NIR goggle (620.P1002.00 Skyline) for the operator.

3.3.9 Welding Experimental Procedure

The experimental procedure can be summarized as:

- Plate preparation (5mm thick x 50 mm width x 200mm long), by horizontal band saw machine and surface grinding machine;
- Positioning of the welding power supply and coordinate welding table;
- Checking the water of cooling water system on power supply;
- Installation of holding system for plates;
- Positioning of electrode wire feeding system;
- Installing of knurled V groove rolls for FCAW process;
- welding torch assembly, including verification of the contact tip and torch angle;
- Assembly of electrode wire (E71T-1 / $\varnothing 1.2$ mm) and adjusting 18 mm for CTWD;
- Installation of shielding gas equipment, including verification and measurement of gas flow (14 lit/min);
- Installation of electrical data transient acquisition system;
- Installation of positioning of near infrared vision system;
- Installation of positioning of digital high speed camera;
- Calibration of control measurement equipment, such as: DAQ system, welding speed, wire feed speed.
- Plate installation and fixing by holding system;
- Adjustment of the wire feed speed, the reference voltage and welding speed;
- Preparation of welding environment;
- Start of welding and start to acquisitioning of the voltage data and current, leaving a time interval to enter the stable welding regime and then turn on the laser and giving the video by high speed camera;
- Analysis of videos, photos and data acquisition.

CHAPTER IV

RESULTS AND DISCUSSION

This chapter presents the results of work study, which obtained by using the methodology that described in Chapter III. As explained, the Table 3.3 shows 108 different tests with different input parameters such as welding speed, wire feed speed and voltage. The principal output of these tests are, the videos and photos which obtained by high-speed camera and also the values of current and voltage which obtained by DAQ system and additional software. Finally the principal purpose of this chapter is discussion about these outputs to find difference types of metal transfer and different group for these tests.

4.1 Metal transfer modes

Due to the presence of flux, metal transfer in FCAW process is different from the GMAW process. The common modes of metal transfer in GMAW are short circuit, globular and spray transfers.

In this study during the gas-shielded flux cored arc welding, the droplet is formed at the tip of the wire and is driven by the flow until the weld pool and depending on the different parameters such as voltage level, wire feed speed and others. Six principal modes of metal transfer could be identified by observing the high-speed camera photos and LabView system as illustrated in Figure 4.1.

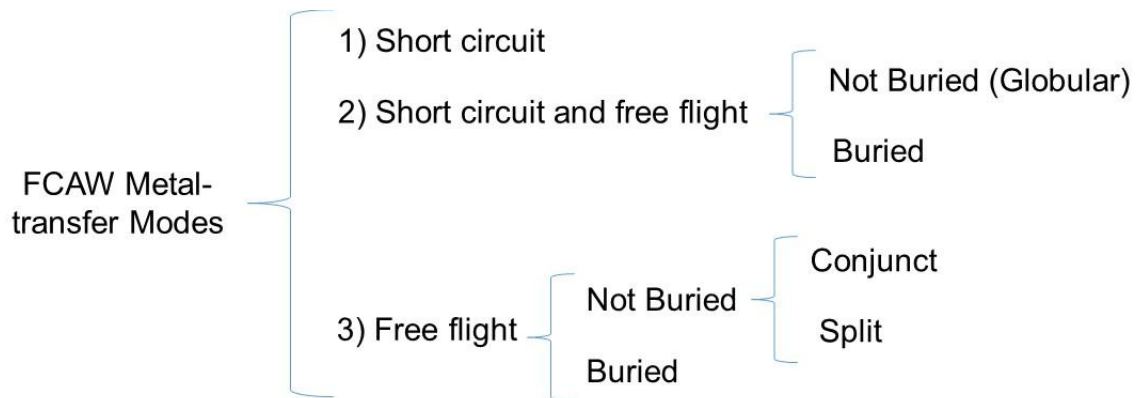


Figure 4.1: Observed and categorized metal-transfer modes during FCAW

As seen in Figure 4.1, it was possible to detect six (6) metal transfer modes in the evaluated conditions:

- ✓ Short circuit (SC);
- ✓ Short circuit and free flight without buried transfer (SC-FF-WOB);
- ✓ Short circuit and free flight with buried transfer (SC-FF-WB);
- ✓ Free flight without buried transfer in conjunct type (FF-WOB-CO);
- ✓ Free flight without buried transfer in split type (FF-WOB-SPL);
- ✓ Free flight with buried transfer (FF-WB).

Moreover, in some tests, stable conditions were not reached and they are identified as non-applicable (NA), as illustrated in Table 4.1. Thus, the region NA is an area in which it was impossible to accomplish tests due the instability of the welding process. Based on the experimental points, the limits between the regions of different modes were outlined for better visualization.

The dynamic balance between the wire feed rate and the melting rate is very important for stable metal transfer. This delicate balance can be upset by small variations in the wire feed rate, the wire extension and voltage, or during transient conditions such as the starts or ends of welds. When the electrode feeding rate is less than its fusion rate, the electrode will fuse back so that its arcing terminal is within the electrode guide. In addition, when the electrode-feeding rate is more than its fusion rate, electrode hits the plate.

Table 4.1: Applicable and non-applicable tests number (input values to power source)

U(v)											
40		100	101	102	103	104	105	106	107	108	
38		91	92	93	94	95	96	97	98	99	
36		82	83	84	85	86	87	88	89	90	
34		73	74	75	76	77	78	79	80	81	
32		64	65	66	67	68	69	70	71	72	
30		55	56	57	58	59	60	61	62	63	
28		46	47	48	49	50	51	52	53	54	
26		37	38	39	40	41	42	43	44	45	
24		28	29	30	31	32	33	34	35	36	
22		19	20	21	22	23	24	25	26	27	
20		10	11	12	13	14	15	16	17	18	
18		1	2	3	4	5	6	7	8	9	
		4	6	8	10	12	14	16	18	20	WFS(m/min)
<div> <div></div> Applicable <div></div> Non applicable </div>											

4.1.1: Short Circuit (SC):

Short circuit transfer occurs when filler metal is deposited from the electrode by short circuiting to the workpiece surface. Also known as dip transfer or short arc, this is an all-positional welding since its low heat input. Parametric settings, along with proper shielding gas selection, determine if welds are produced with short circuit transfer. The use of relatively low current and arc voltage setting cause the electrode to intermittently short circuit with the weld pool at a controlled frequency. Metal is transferred by the wire tip actually dipping into the weld pool and finally a short circuit mode will happen. In this type of metal transfer the movement of electrode is very high which cause to have a different arc length and a big value of standard deviation for arc lengths.

In Table 4.2 shows all the tests with the short circuit characteristics. Also Figures 4.1.1 and 4.1.2 show an example of voltage and current signals and photos for a short circuit transfer mode which occurred in run 39.

Table 4.2: Set value and monitoring results for short circuit mode

Run	Ur (V)	WFS (m/min)	Ws (cm/min)	Im (A)	Irms (A)	Um (V)	Urms (V)	La (mm)
10	20	4.0	9.1	140	159	15.7	17.6	1.2±0.9
19	22	4.0	9.1	140	152	18.1	19.4	2.1±1.0
20	22	6.0	13.6	186	202	16.8	18.8	1.5±1.0
29	24	6.0	13.6	197	210	18.8	20.5	2.7±1.3
30	24	8.0	18.2	232	247	18.3	20.3	2.4±1.5
31	24	10.0	22.7	263	285	17.0	19.4	1.1±0.9
32	24	12.0	27.3	278	301	16.2	18.6	1.3±0.8
33	24	14.0	31.8	307	326	16.2	18.5	1.6±1.4
39	26	8.0	18.2	230	243	20.0	21.7	2.2±1.8
40	26	10.0	22.7	272	285	19.2	20.9	1.3±0.7
41	26	12.0	27.3	283	300	18.8	20.6	1.8±1.4
42	26	14.0	31.8	312	330	17.1	19.2	1.9±1.4
43	26	16.0	36.4	339	352	16.2	18.1	1.4±1.3
49	28	10.0	22.7	272	281	20.8	22.4	1.6±1.0
50	28	12.0	27.3	285	298	19.9	21.6	1.4±1.0
51	28	14.0	31.8	303	322	19.2	21.0	1.4±1.1
52	28	16.0	36.4	337	350	17.9	19.8	1.8±1.4
59	30	12.0	27.3	289	297	22.3	23.6	1.7±1.1
60	30	14.0	31.8	310	321	21.3	22.5	2.4±1.7
61	30	16.0	36.4	328	340	20.5	21.8	1.8±1.6
62	30	18.0	40.9	359	369	18.8	20.3	0.9±0.8

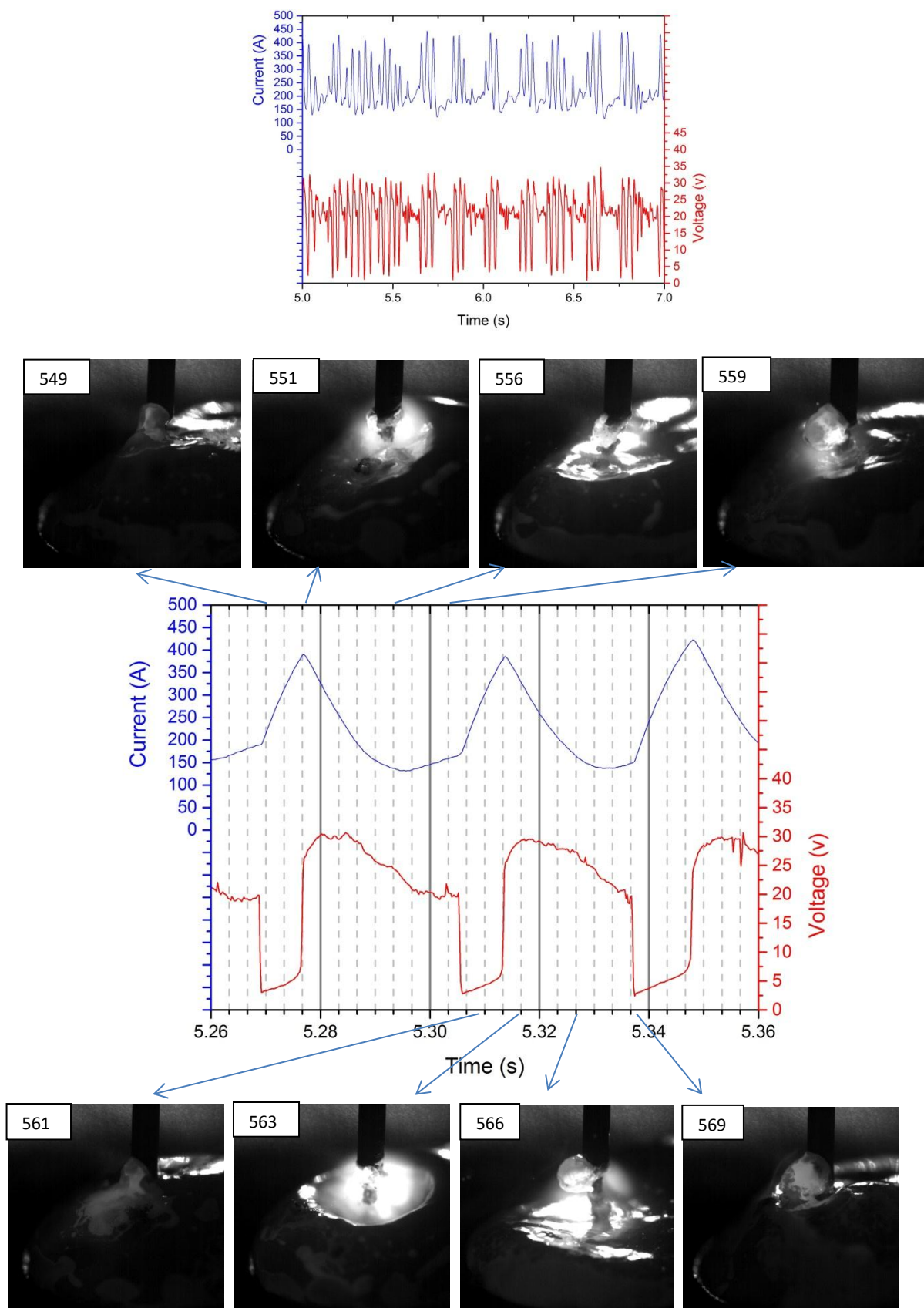


Figure 4.1.1: Voltage and current signals for a short circuit metal transfer-(Run 39)

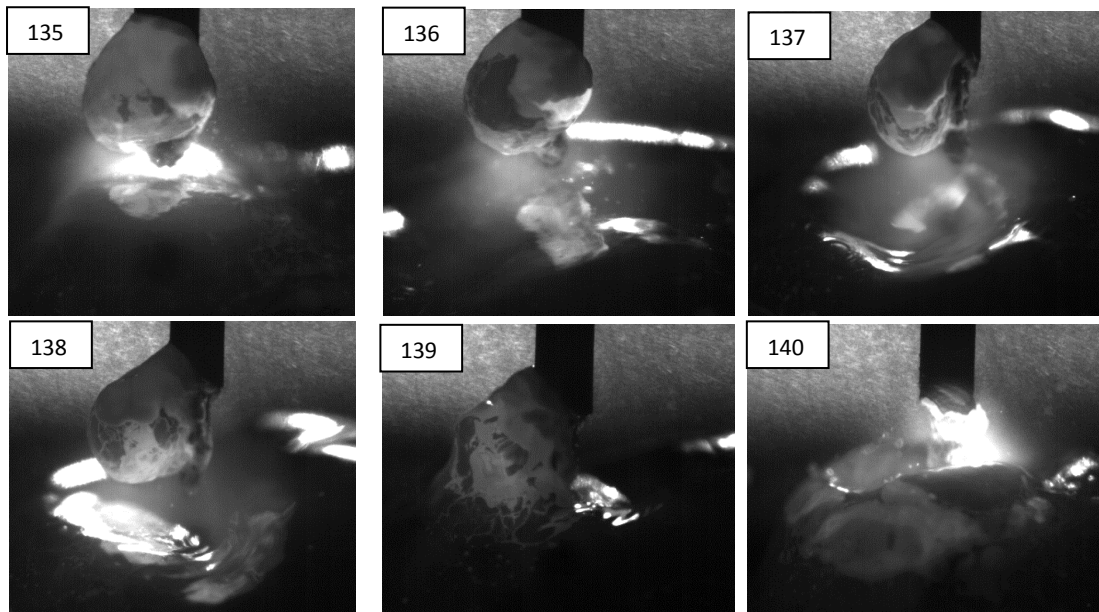


Figure 4.1.2: Image sequence captured during FCAW in a short circuit transfer mode- (Run 39)

4.1.2 Short circuit and free flight (transition area):

As explained in literature review, the free flight metal transfer generally occurs at high current and high arc voltage ranges, so with increasing the heat input, after short circuit, free flight metal transfer occurs. Moreover, during the use of FCAW / GMAW process, there is a transition area where short circuiting transfer end and free flight transfer begins. In these areas, short circuit and free flight metal transfer occur with together before completely all the metal transfer changed to free flight type. Figure 4.1.3 shows an example of a voltage and current signals for a short circuit and free flight metal transfer type, which occurred in run 28. During this type of metal transfer electrode stick out just changes a little and the droplets grows sufficiently to touch the pool. This growing droplet sometimes can reach a large size to have a short circuit type and sometimes can be smaller to have a free flight metal transfer the is without touch the pool.

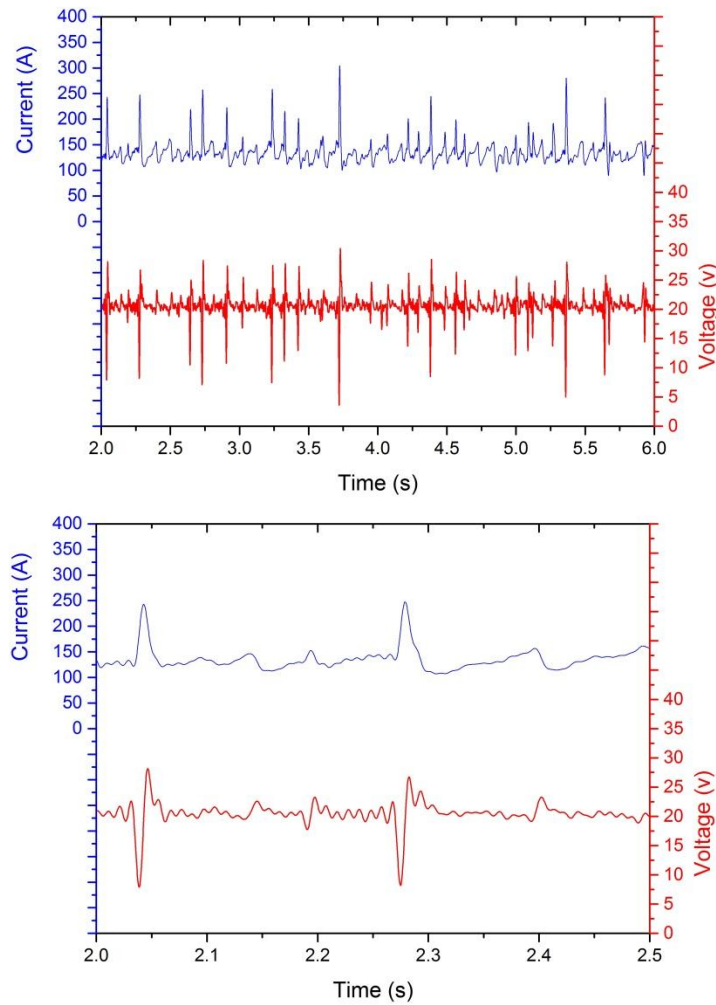


Figure 4.1.3: Voltage and current signals for a short circuit and free flight metal transfer- (Run 28)

In this study by observing of photos and videos captured by high-speed camera, it can divide this group in two more different groups, which are:

- ✓ Short circuit and free flight without buried (SC-FF-WOB)
- ✓ Short circuit and free flight with buried (SC-FF-WB)

The buried and not buried conditions can explained in this study as follow. When the arc length is very small and tip of the electrode is on the weld pool and metal transfers occur in the distance between the surface of plate and surface of weld bead, the transfer is called “with buried”, which it is difficult to observe the metal transfer. On the other way, when tip of the electrode is far from the weld pool, and metal transfer not occur in that distance, it called “without buried”, as illustrated in Figure 4.1.4.

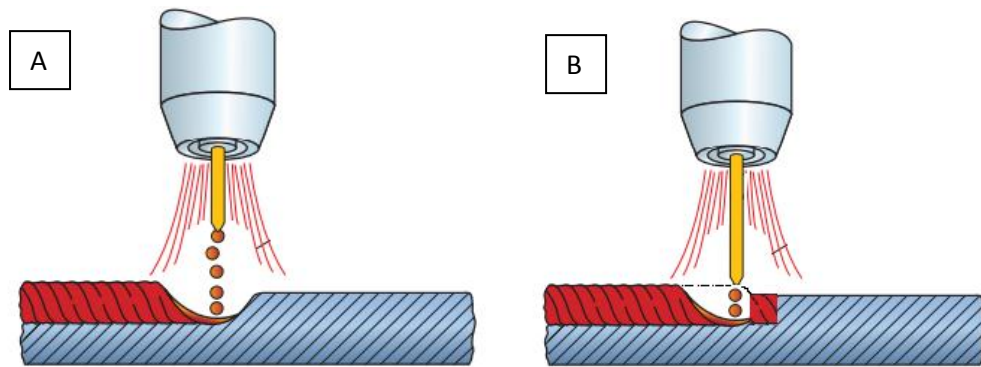


Figure 4.1.4: Schematic electrode positioning for A) without buried and B) with buried metal transfer type

4.1.2.1 Short circuit and free flight without buried (SC-FF-WOB):

Generally by increasing the voltage at the same wire feed speed, the arc length will increase too. Thus, it is the principal reason why the metal transfer mode changes to free flight from short circuit, but in this type of metal transfer tip of electrode is not very far from molten pool surface and is not very near neither. Also the molten pool has a lot of movement, so cause of these, the drop of electrode, sometimes transferred by short circuiting and sometime without it, which is free flight type. The Table 4.3 shows all the tests with the short circuit and free flight metal transfer type without buried characteristics

Table 4.3: Set value and monitoring results for short circuit and free flight without buried (SC-FF-WOB)

Run	Ur (V)	WFS (m/min)	Ws (cm/min)	Im (A)	Irms (A)	Um (V)	Urms (V)	La (mm)
28	24	4.0	9.1	135	137	20.5	20.7	2.3±0.8
38	26	6.0	13.6	189	190	21.0	21.4	2.1±0.7
47	28	6.0	13.6	190	190	23.0	23.1	2.0±0.4
48	28	8.0	18.2	231	234	22.5	22.9	2.2±0.9
57	30	8.0	18.2	233	234	23.7	23.9	2.3±0.5
58	30	10.0	22.7	263	265	23.2	23.7	1.9±0.6
67	32	10.0	22.7	267	267	25.0	25.1	2.0±0.5
68	32	12.0	27.3	288	289	24.7	25.1	2.2±1.0
69	32	14.0	31.8	310	314	23.3	24.0	1.6±0.6
76	34	10.0	22.7	264	264	26.5	26.6	2.1±0.5

Figure 4.1.5 shows an example of a FCAW images sequence for a short circuit and free flight mode without buried (SC-FF-WOB), which occurred in test number 48 where in images 204, 205 and 206 one can see a short circuit metal transfer and in images 253, 254 and 255 one can see a free flight metal transfer and also in images 286, 287 and 288 one can see a short circuit metal transfer just by the inner flux.

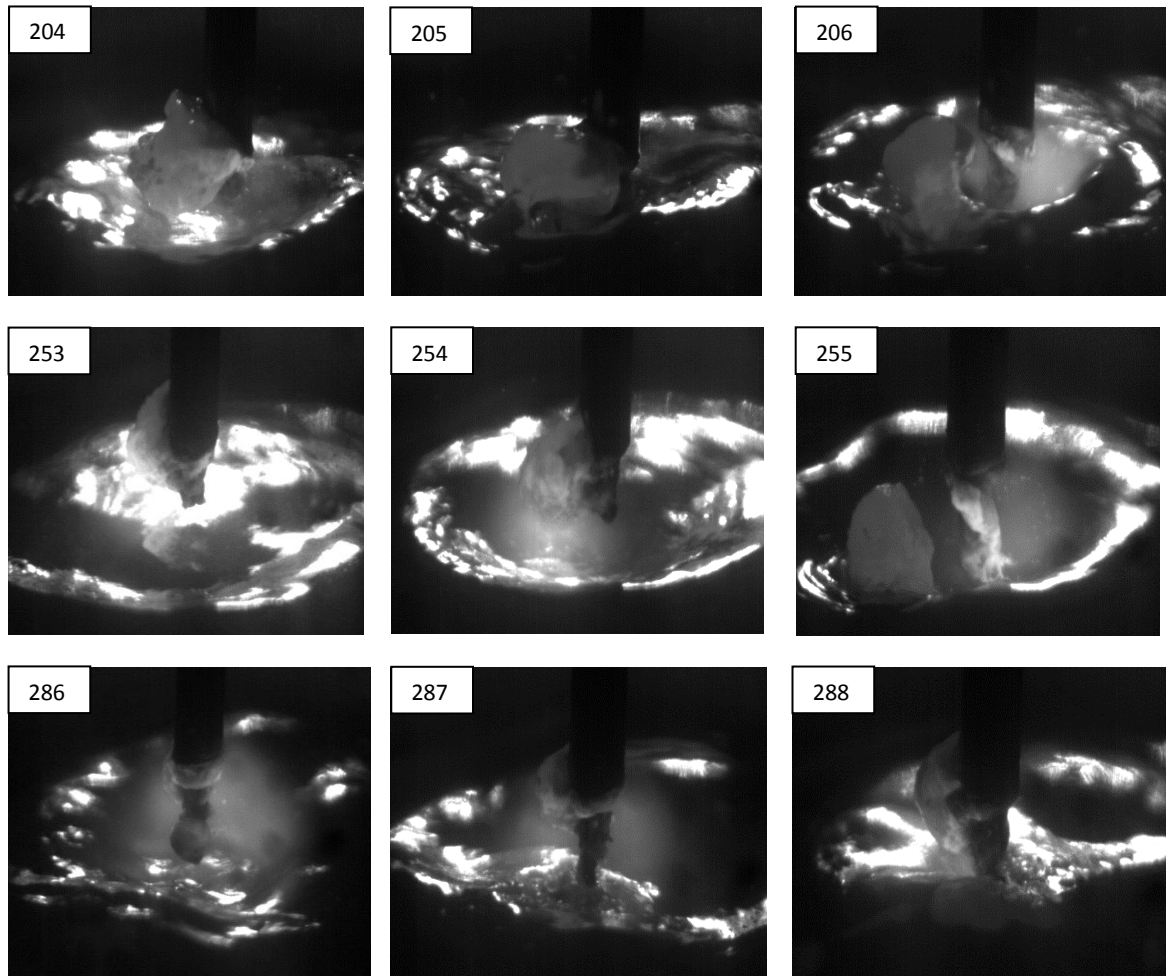


Figure 4.1.5: Image sequence captured during FCAW in a short circuit and free flight mode without buried (SC-FF-WOB)-(Run 48)

4.1.2.2 Short circuit and free flight with buried (SC-FF-WB):

As previously explained, for a short circuit and free flight mode with buried (SC-FF-WB), the electrode tip is on the weld pool and occur turbulence system on there. This metal

transfer happened when increased wire feed speed at the approximately same voltages utilized for SC-FF-WOB metal transfer type.

When metal transfer happened with buried type, actually one cannot see how drop of electrode transfers to molten pool, but because of the movement of molten pool just in a few images can see some drop of metal transfer with free flight type. Moreover, in this type of metal transfer, a short circuit happened when the molten pool completely surrounds the electrode, close the molten pool area and cut the electrode and again happened a new arc. The Table 4.4 shows all the tests with the short circuit and free flight metal transfer type with buried characteristics.

Table 4.4: Set value and monitoring results for short circuit and free flight with buried (SC-FF-WB)

Run	Ur (V)	WFS (m/min)	Ws (cm/min)	Im (A)	Irms (A)	Um (V)	Urms (V)	La (mm)
70	32	16.0	36.4	332	335	23.5	23.9	1.2±0.8
71	32	18.0	40.9	362	367	21.3	22.3	1.1±1.0
72	32	20.0	45.5	365	368	21.7	22.5	1.0±1.1
78	34	14.0	31.8	314	315	25.8	26.1	1.2±0.6

Figure 4.1.6 shows an example of a FCAW images sequence for a short circuit and free flight mode with buried (SC-FF-WB), which occurred in run 71 where in images 144,145 and 146 can see a free flight metal transfer and in images 149,148 and 150 can see molten pool completely surrounds the electrode and close the molten pool area.

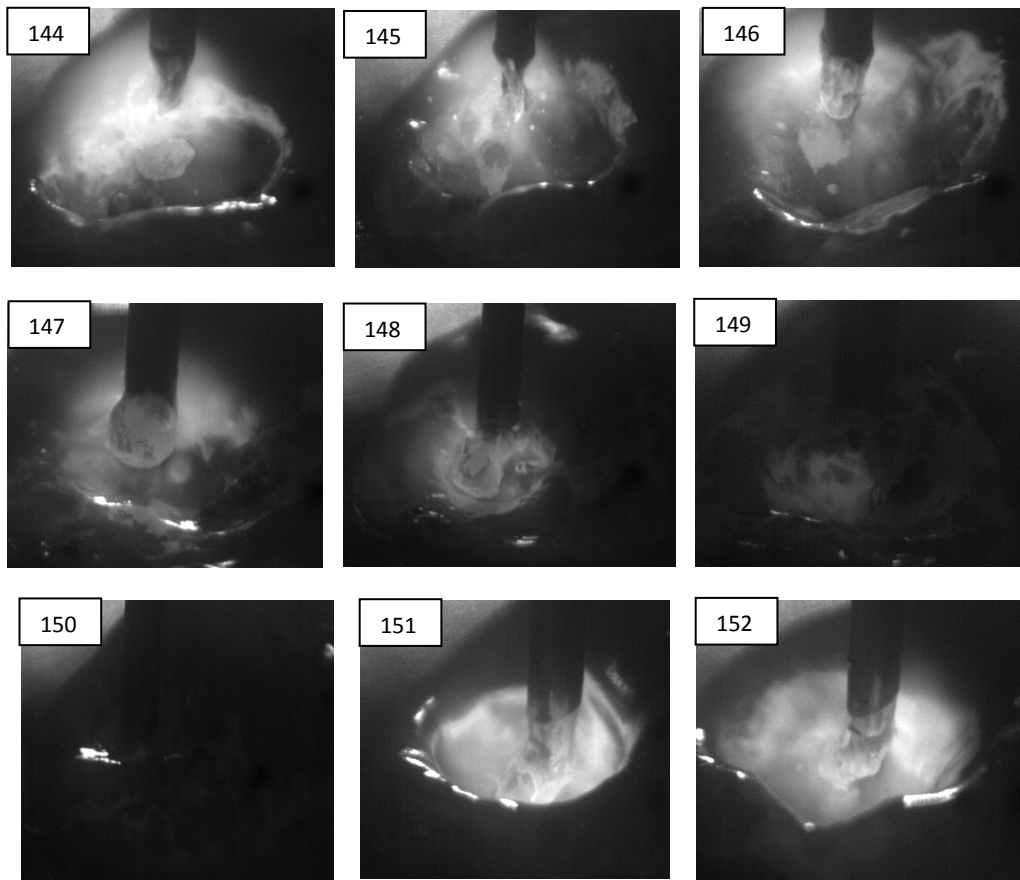


Figure 4.1.6: Image sequence captured during FCAW in a short circuit and free flight mode with buried (SC-FF-WB)-(Run 71)

4.1.3 Free Flight:

As the name implies, free-flight transfer involves complete detachment of the molten metal drop from the consumable electrode and, then, its flight to the workpiece and weld pool, without any direct physical contact. During this flight, the drops are free of both the consumable electrode and the workpiece. This type of metal transfer occurs in high voltage where, passed the transition region and all the drops of electrode just transferred with free flight type. In Figure 4.1.7, shows an example of voltage and current signals for a free flight metal transfer type, which occurred in run 55.

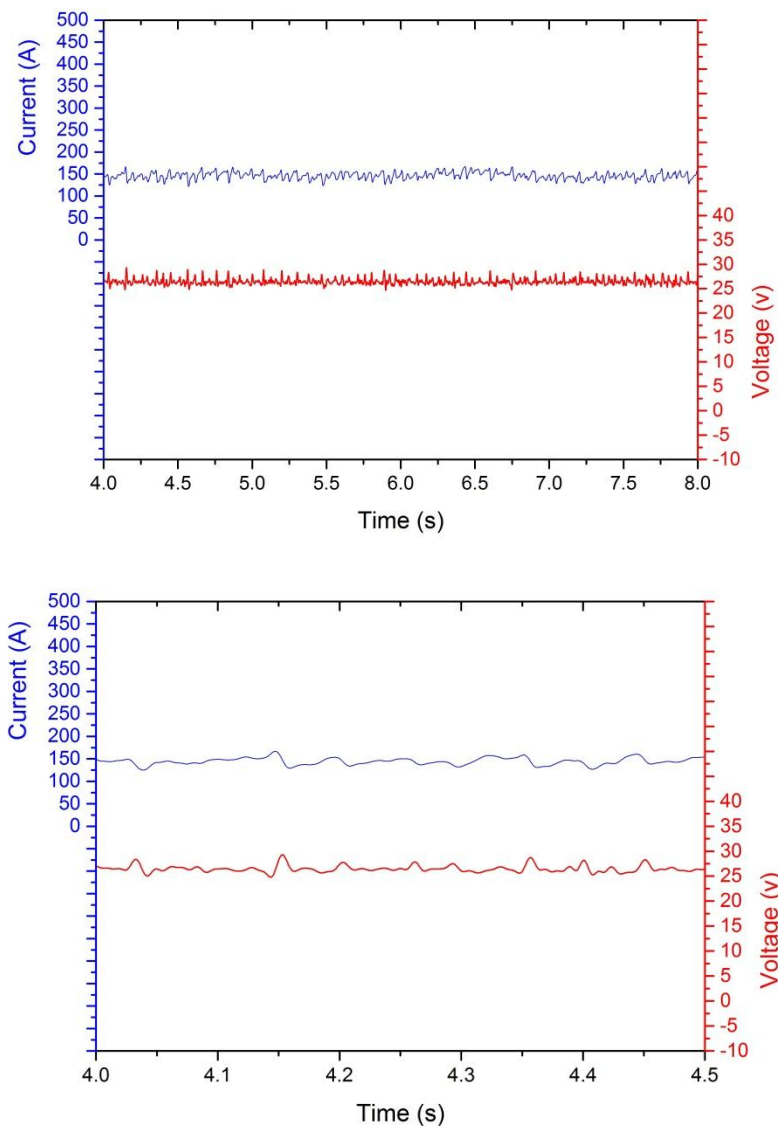


Figure 4.1.7: Voltage and current signals for a free flight metal transfer-(Run 55)

This group by observing of photos and videos can divided in three more detail groups which are:

- ✓ Free flight without buried in conjunct type (FF-WOB-CO),
- ✓ Free flight without buried in split type (FF-WOB-SPL),
- ✓ Free flight with buried (FF-WB),

To understand better about the conjunct and split metal transfer type, can explained that, in this study when the part of flux and steel of electrode, transferred separated it called split and if they transferred with together, it called conjunct, as illustrated in Figure 4.1.8.

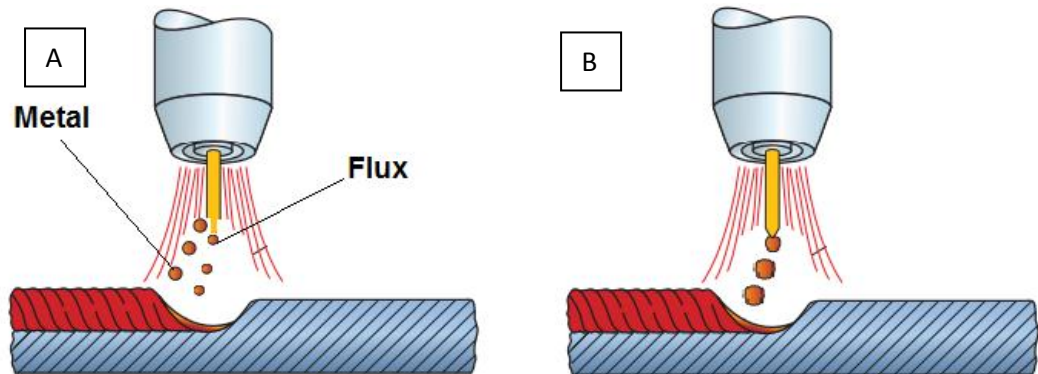


Figure 4.1.8: Schematic of metal transfer for A) Split type and B) Conjunct

4.1.3.1 Free flight without buried in conjunct type (FF-WOB-CO)

This type of metal transfer occurs in high voltage but low current (in the range of 50-150 A). The molten metal started to fall down from the solid part of the electrode and will join with the flux part of the electrode and is transferred in the form of drops that have a diameter larger than the wire. These large drops form at the electrode tip and detach, largely due to the force of gravity, like water dripping from a tap. Once detached, these large drops fall through the arc column into the molten weld pool to be taken up by surface tension forces. The rate of drop or globule formation, detachment, and transfer is relatively slow. This mode of transfer is like as globular or drop transfer in MIG/MAG process by a different which in MIG/MAG process there is not any flux. The table 4.5 shows all the tests with the free flight metal transfer without buried in conjunct type characteristics.

Figure 4.1.9 shows an example of a FCAW images sequence for a free flight mode without buried in conjunct type (FF-WOB-CO), which occurred in run 46.

Table 4.5: Set value and monitoring results for free flight metal transfer without buried in conjunct type (FF-WOB-CO)

Run	Ur (V)	WFS (m/min)	Ws (cm/min)	Im (A)	Irms (A)	Um (V)	Urms (V)	La (mm)
37	26	4.0	9.1	136	137	22.4	22.4	2.2±0.5
46	28	4.0	9.1	140	140	24.2	24.2	3.0±0.4
55	30	4.0	9.1	146	146	26.4	26.4	3.3±0.4
56	30	6.0	13.6	194	194	25.0	25.1	2.7±0.4
64	32	4.0	9.1	141	141	27.7	27.7	4.4±0.4
66	32	8.0	18.2	238	239	25.7	25.8	2.5±0.3
73	34	4.0	9.1	143	143	29.7	29.7	4.9±0.7
82	36	4.0	9.1	145	145	31.6	31.6	5.4±0.4
91	38	4.0	9.1	149	149	33.4	33.4	6.2±0.4
100	40	4.0	9.1	150	151	35.5	35.5	6.7±0.3

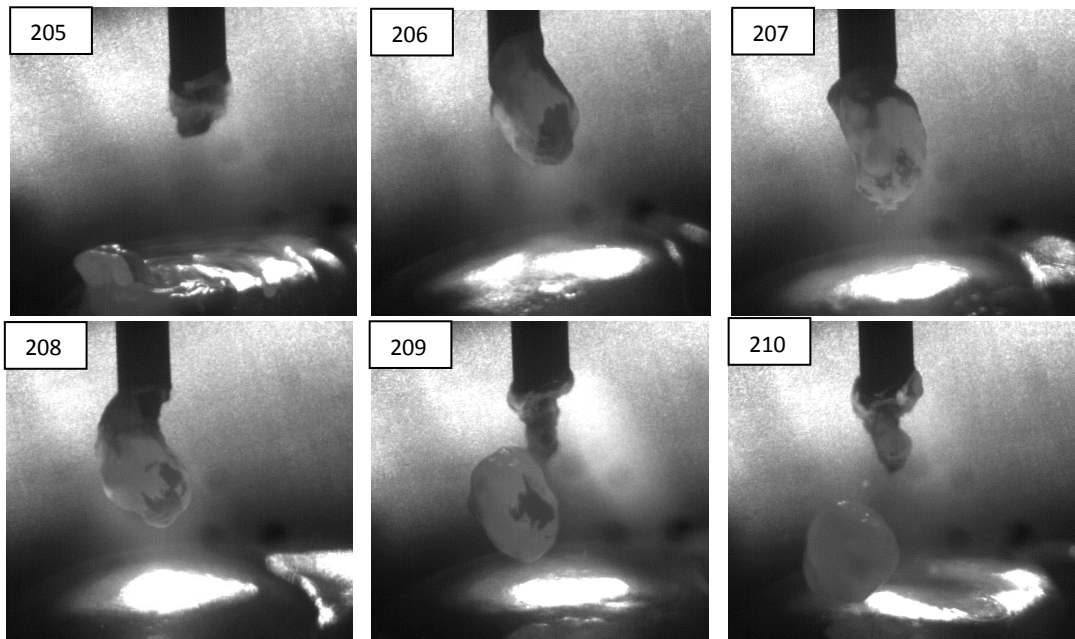


Figure 4.1.9: Image sequence captured during FCAW in a free flight mode without buried in conjunct type (FF-WOB-CO)-(Run 46)

4.1.3.2 Free flight without buried in split type (FF-WOB-SPL)

After FF-WOB-CO type of metal transfer by increasing the wire feed speed, current and finally heat input will increase too. Cause of these, the molten metal which started to fall down from the solid part of the electrode, before being join with the flux part of the electrode because of high level of energy, will separate faster and transfers separately in the molten weld pool and also the flux part of the electrode will transfer separately too. During of this metal transfer type sometimes they get accident with together (drops of solid part with drops of flux part) so because of this, will happened lots of splash during metal transfer. The table 4.6 shows all the tests with the free flight metal transfer without buried in Split type characteristics

Table 4.6: Set value and monitoring results for free flight metal transfer without buried in split type (FF-WOB-SPL)

Run	Ur (V)	WFS (m/min)	Ws (cm/min)	Im (A)	Irms (A)	Um (V)	Urms (V)	La (mm)
65	32	6.0	13.6	193	193	27.0	27.1	3.5±0.4
74	34	6.0	13.6	197	198	28.7	28.8	4.4±0.3
75	34	8.0	18.2	232	232	27.6	27.8	3.4±0.3
77	34	12.0	27.3	302	302	26.5	26.6	2.3±0.3
83	36	6.0	13.6	197	197	30.6	30.7	5.8±0.5
84	36	8.0	18.2	241	241	29.6	29.7	5.1±0.4
85	36	10.0	22.7	267	267	29.2	29.3	3.0±0.5
86	36	12.0	27.3	292	292	28.3	28.6	2.8±0.4
87	36	14.0	31.8	317	317	27.7	27.9	2.3±0.5
92	38	6.0	13.6	205	205	32.5	32.5	6.3±0.2
93	38	8.0	18.2	243	241	31.2	31.4	5.5±0.7
94	38	10.0	22.7	273	273	30.7	30.8	4.3±0.3
95	38	12.0	27.3	297	297	30.2	30.3	3.4±0.6
96	38	14.0	31.8	319	320	29.1	29.3	2.8±0.3
101	40	6.0	13.6	208	208	34.5	34.6	7.2±0.3
102	40	8.0	18.2	251	251	33.1	32.9	6.0±0.3
103	40	10.0	22.7	278	278	32.4	32.6	5.1±0.3
104	40	12.0	27.3	303	303	31.5	31.7	3.9±0.3
105	40	14.0	31.8	324	325	30.9	31.2	3.1±0.4

Also Figure 4.1.10 shows an example of a FCAW images sequence for a free flight mode without buried in split type (FF-WOB-SPL), which occurred in run 102.

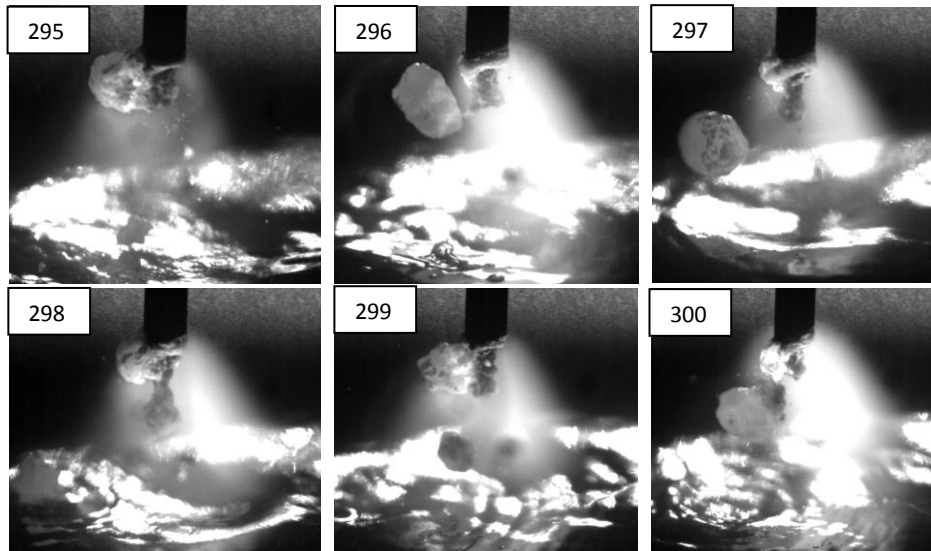


Figure 4.1.10: Image sequence captured during FCAW in a free flight mode without buried in split type (FF-WOB-SPL)-(Run 102)

4.1.3.3 Free flight with buried (FF-WB)

The latest classified metal transfer mode is free flight one with buried electrode that happened in high voltage, high wire feed speed and high current. It means it happened in high level of welding energy. As the name implies, in free flight transfer with buried, tip of electrode is on the weld pool. Thus, one cannot see very well how the drops transfer, but because of the signals of each tests, which illustrated in Figure 4.1.7, it is possible to understand that this type of metal transfer is free flight. However, because of the movement of molten pool and electrode during the welding, just in a few images can see some drop of metal transfer. The Table 4.7 shows all the tests with the free flight metal transfer with buried characteristics.

Figure 4.1.11 shows two example of a FCAW images sequence for free flight mode with buried (FF-WB), which occurred in run 88 and 79.

Table 4.7: Set value and monitoring results for free flight metal transfer with buried (FF-WB).

Run	Ur (V)	WFS (m/min)	Ws (cm/min)	Im (A)	Irms (A)	Um (V)	Urms (V)	La (mm)
79	34	16.0	36.4	335	335	25.7	25.8	1.9±0.4
80	34	18.0	40.9	351	351	25.6	25.6	1.4±0.5
81	34	20.0	45.5	365	366	24.4	24.7	1.2±0.5
88	36	16.0	36.4	341	341	27.7	27.8	2.0±0.5
89	36	18.0	40.9	362	362	27.1	27.1	1.3±0.4
90	36	20.0	45.5	374	374	27.0	27.0	1.0±0.3
97	38	16.0	36.4	345	345	29.4	29.5	2.4±0.5
98	38	18.0	40.9	371	371	28.6	28.6	1.9±0.5
99	38	20.0	45.5	384	384	28.4	28.5	1.4±0.3
106	40	16.0	36.4	344	344	31.4	31.5	3.0±0.8
107	40	18.0	40.9	373	373	31.0	31.0	2.6±0.3
108	40	20.0	45.5	394	394	30.6	30.7	1.8±0.5

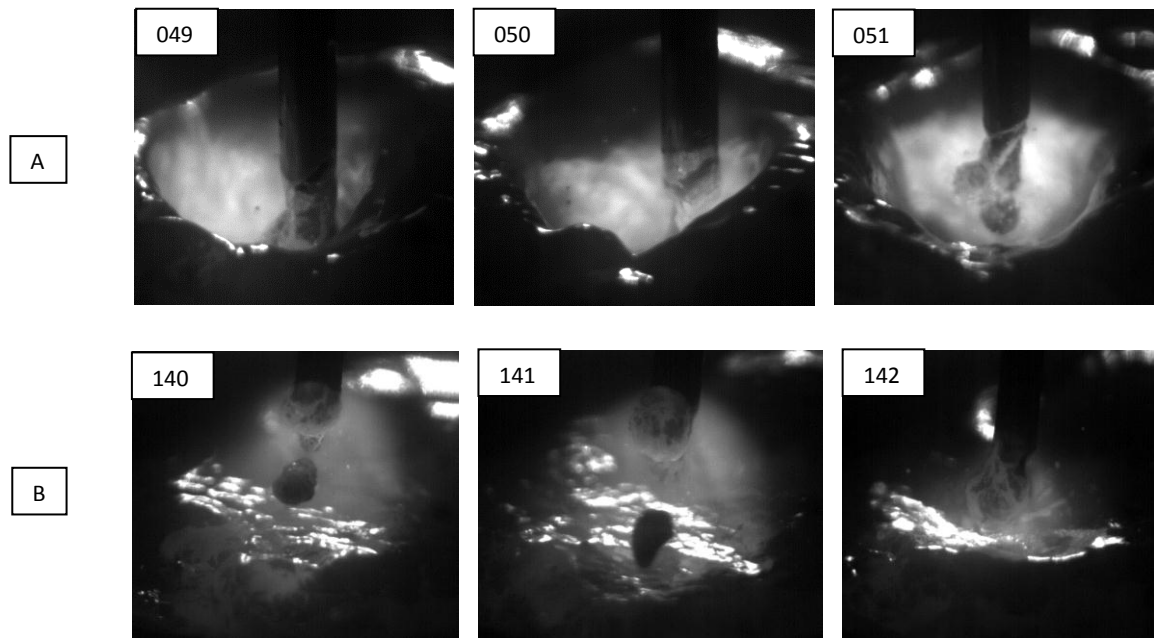


Figure 4.1.11: Image sequence captured during FCAW in a free flight mode with buried (FF-WB) A) Run 88 B) Run 79

4.2 Presentation of metal transfer maps

Metal transfer maps are diagrams that show regions where different modes of metal transfer occur as a function of mean voltage with wire feed speed and arc length with welding current. Many studies for monitoring the transfer modes have already been performed by using different conditions of welding and different materials.

In this study, the focus was to investigate the metal transfer mode and to establish the boundaries of the different transfer modes for FCAW (DC+) process with the electrode E71T-1 ($\varnothing 1.2\text{mm}$), 18 mm CTWD and Ar+25%CO₂. Figure 4.2.1 shows the compilation of the presented metal-transfer modes as a function of mean voltage with wire feed speed. It must be pointed out that current should not be considered as an independent variable in FCAW, when using power sources with constant-voltage characteristics. Wire feed rate is the true independent variable. Current should be considered with arc length with illustrated in Figure 4.2. The wire feed rate depends only on the wire feeder control setting since the power for the wire feeder is separate from the power supplied for welding. Therefore, new metal transfer maps were plotted as a function of welding voltage and wire feed.

Therefore, in order to provide additional information for the physical phenomena, Figure 4.2.2 presents the metal transfer map as a function of arc length versus current, using the characteristics and transfer mode nomenclature presented in Section 4.1.

Such final results are in general agreement with literature, since overall results define low-voltage characteristic for short circuit mode and high-voltage characteristic for free-flight mode. At this point, Figure 4.2.3 exemplifies the arc length variation measured frame by frame for different runs. For instance, Run 31 clearly shows the arc-length variation characteristic related to short circuit metal transfer. On the other hand, Runs 64, 87 and 99 present arc-length measures that not reach zero, i.e., they are in free-flight mode.

The new insight and main contribution found in this work is defined by the new classification proposed when observing the metal transfer by using the infrared illumination. It is expected that such results can contribute to further discussion about the metal transfer during FCAW.

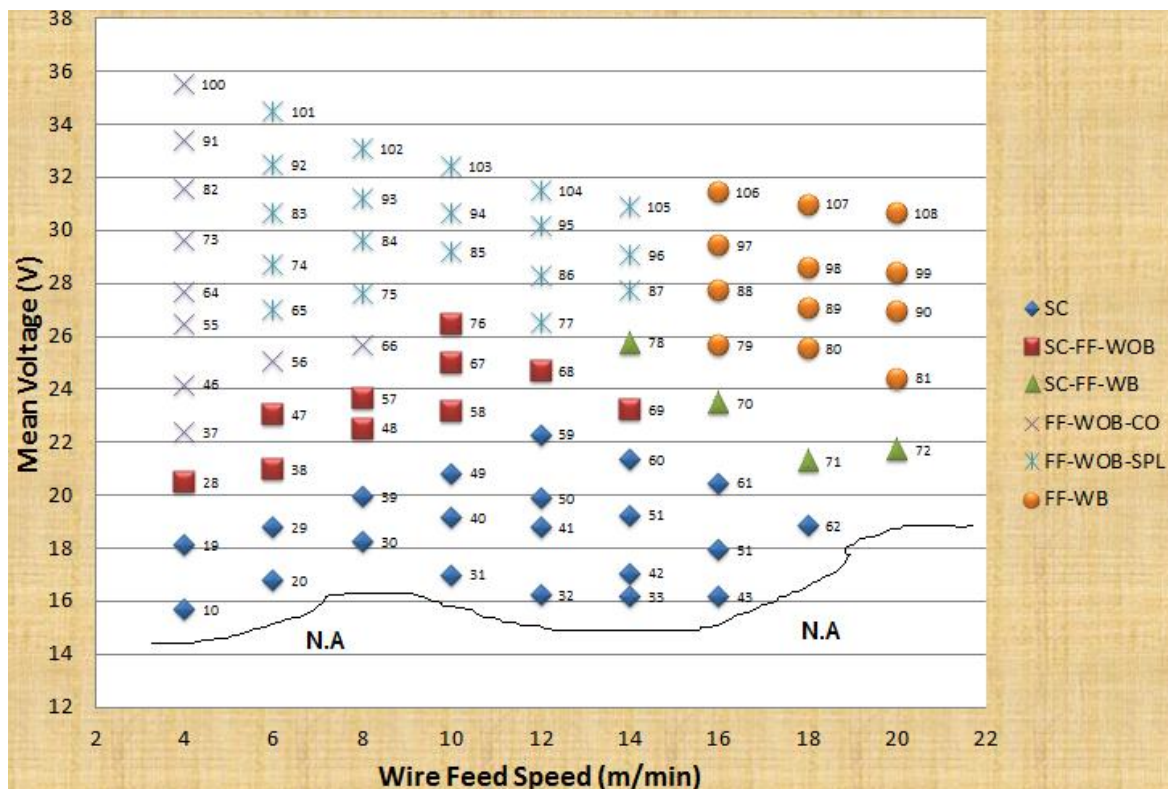


Figure 4.2.1: Map of metal transfer modes in FCAW process as a function of mean welding voltage and wire feed speed.

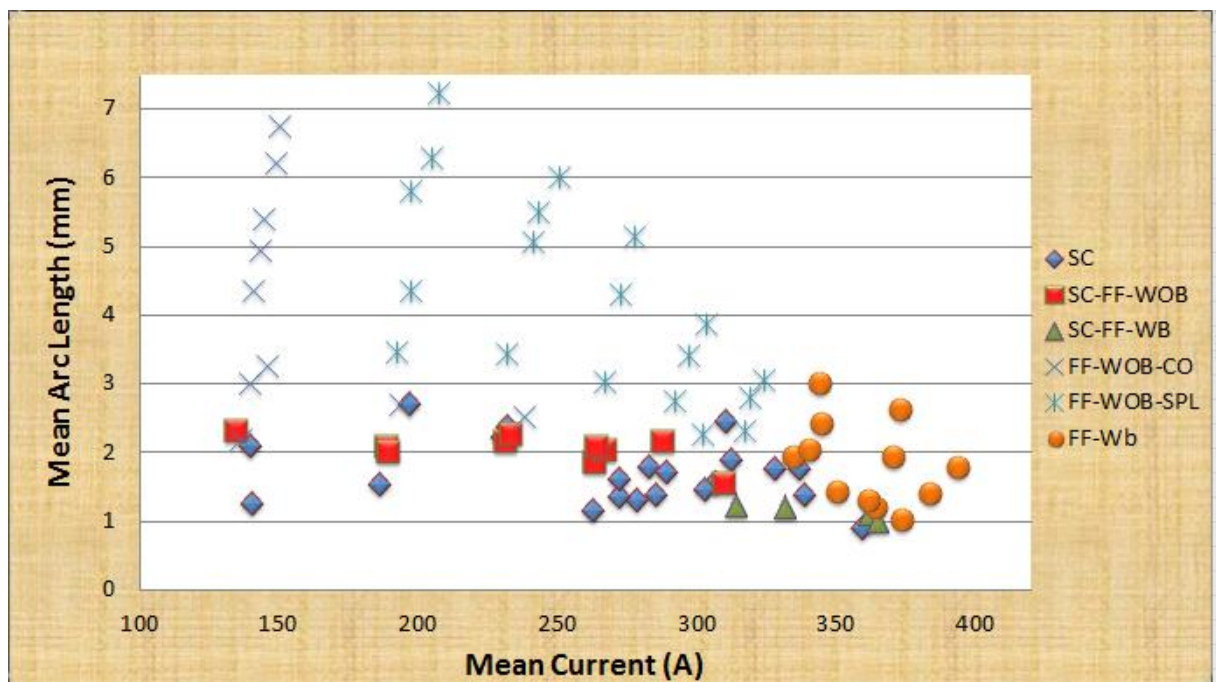


Figure 4.2.2: Map of metal transfer modes in FCAW process as a function of mean arc length and mean current

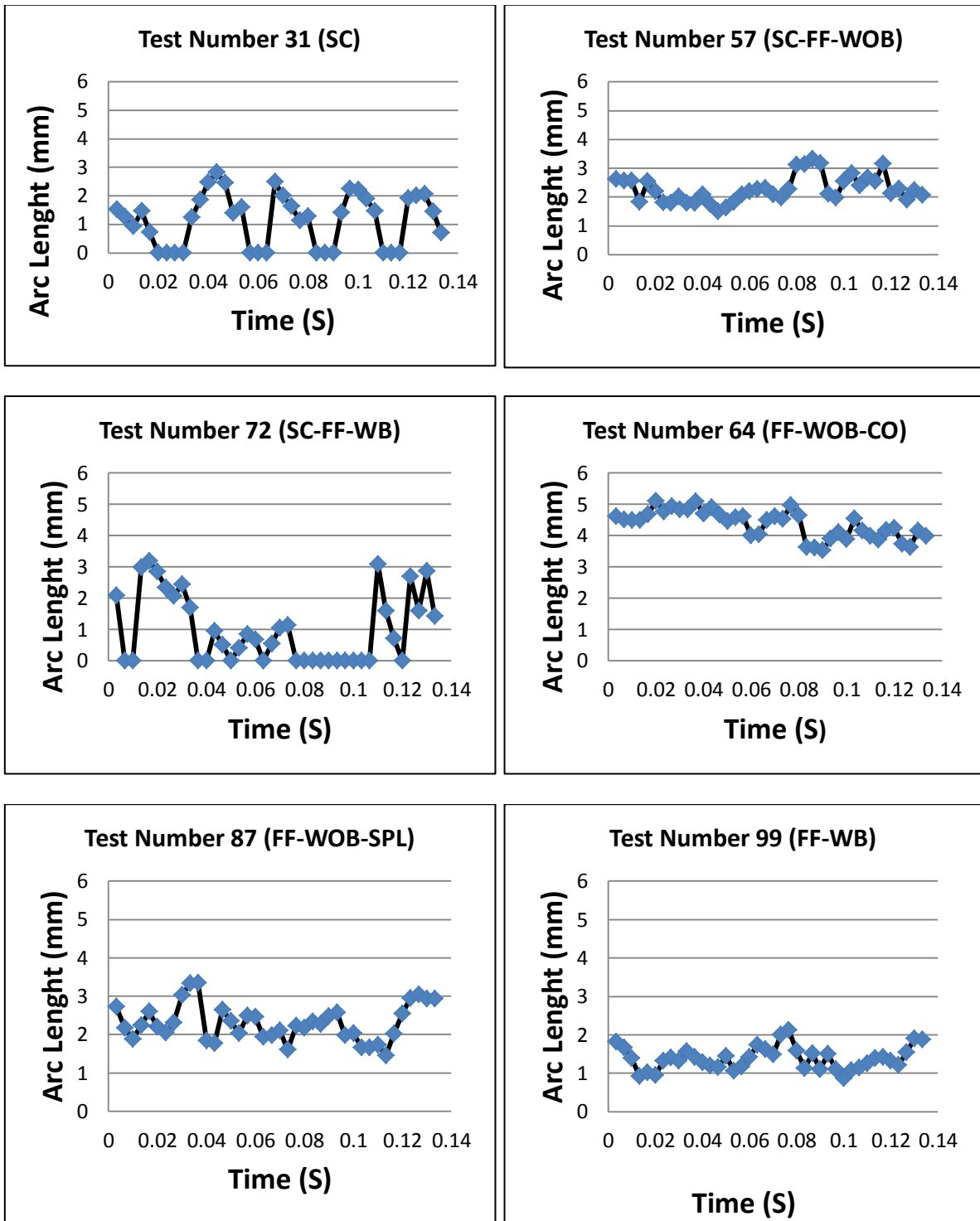


Figure 4.2.3: Arc length variation observed in the images for different runs

CHAPTER V

Conclusion

Flux cored arc welding is widely used in the manufacturing industry, such as automotive, aerospace, and shipbuilding. Metal transfer is a very important issue, and a good understanding of this process will benefit the application of FCAW. According to the results of this investigation, the major conclusions are presented as follows:

A method for visualization of metal transfer in FCAW has been successfully employed. The laser diode based vision system is capable of producing high quality, real-time images of the FCAW processes. The vision system was capable of overcoming the arc light and provide images of the weld area unlike previous studies, which used shadowgraph technique without any image treatment.

The proposed methodology for determining the arc length was adequate, making it a very valuable tool for studies related to the variation of the arc length, such as the study of variation of the arc length due to the use of different metal transfer modes.

Six sub-classifications of metal transfer was found in clearly defined regions on transfer mode map, as summarized in Figure 5.1. This six major metal transfer modes were found in FCAW are:

- ✓ Short circuit (SC);
- ✓ Short circuit and free flight without buried (SC-FF-WOB);
- ✓ Short circuit and free flight with buried (SC-FF-WB);
- ✓ Free flight without buried in conjunct type (FF-WOB-CO);
- ✓ Free flight without buried in split type (FF-WOB-SPL);
- ✓ Free flight with buried (FF-WB).

Also it was found the regions where it was not possible to weldment (N.A), because the welding tests point was highly unstable.

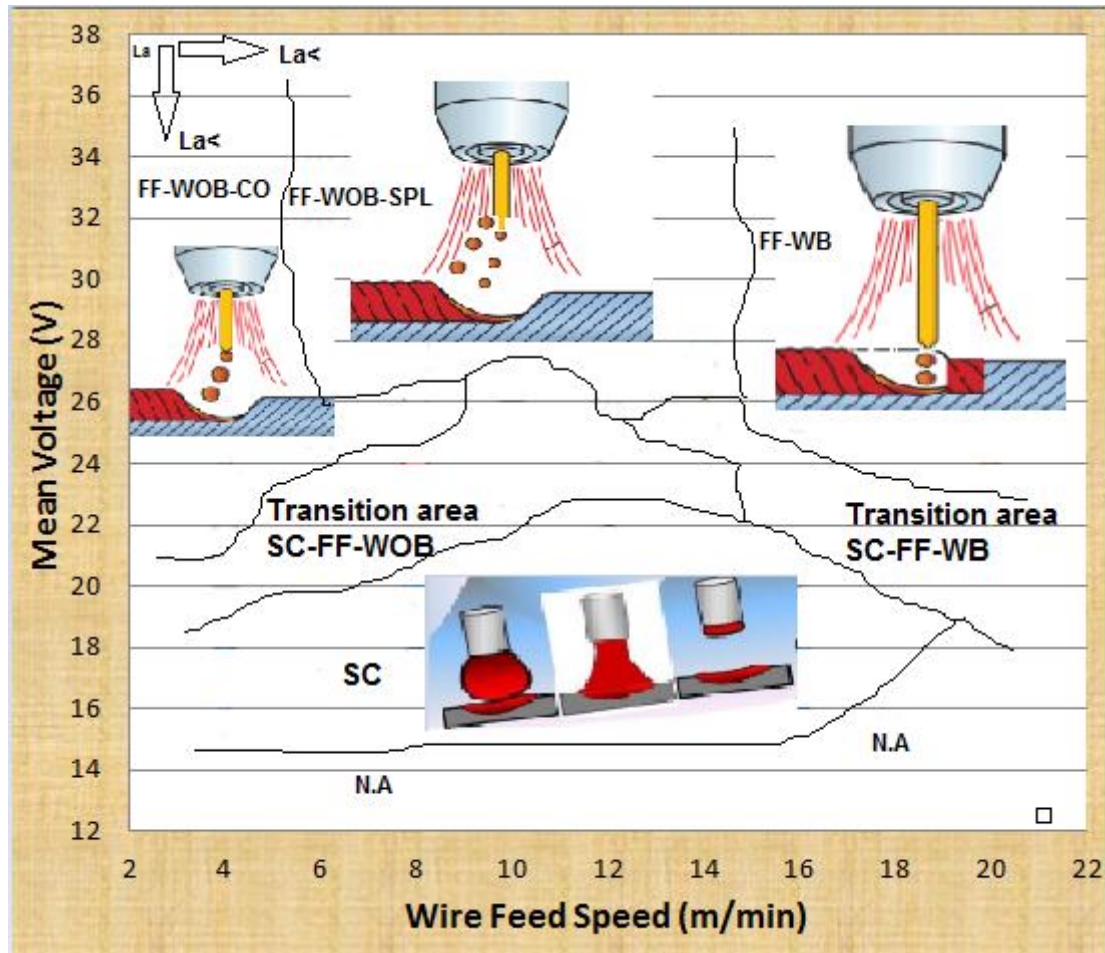


Figure 5.1: Schematic map of the metal transfer modes in FCAW process as a function of wire feed speed and voltage (L_a is the arc length)

Based on these suggestions, a new metal transfer mode classification structured both on the increase of the wire feed speed and voltage (arc length and current) and on the physics of the transfer was proposed for the fundamental transfer modes. It would allow to clearly understanding the relation between the process parameters and metal transfer modes.

CHAPTER VI

Improvements – Future Work

Based on the results and experience gained during this development work, it is believed that the values and behavior some variables, as well as aspects of the process still need better understanding and/or new approach. Therefore, as consequences of this work, it is suggested the following future studies:

Expand the aggregating data of metal transfer modes and maps for FCAW process by regarding the characteristics of:

- ✓ Different steels and alloy as a metal base;
- ✓ Different gas type as a shielding or protection;
- ✓ Different electrode diameter and chemical composition;
- ✓ Different joint type and chamfer type;
- ✓ Different CTWD;
- ✓ Different welding position;
- ✓ Different torch angle;
- ✓ SS-FCAW, double FCAW wire electrode and hybrid laser FCAW.

It is also important to correlate the metal transfer modes with detailed analysis of the microstructure of ZTA and molten zone and also mechanical tests, such as tensile, bending and Charpy in different metal transfer mode, and promote a comparative analysis between them.

Another improvement of the system would be to increase the sampling rate of the frames. In this study, it was used 300 fps for ViaSolda but generally almost need 2000 fps for monitoring of metal transfer. Also can increase the number of laser diodes.

Some other cameras could be performed. An infrared camera, for example, could be used for detecting spatters during a weld. Besides that, more than one camera could be integrated to the system, offering a better visual analysis of the welding phenomena.

The sound emitted by the arc would be another interesting aspect for remote monitoring. Listening to this sound, the feeling of the welder is increased. Besides that, the metal transfer mode could be identified by audio signal analysis.

Another approach is to use the metal transfer map for emulating control strategies for FCAW.

Finally, it is suggested to further review the MIG/MAG metal-transfer modes to include this new classification (with buried and without buried). Depending of parameters and the balance of deposition rate, it is possible to have buried transfer mode in MIG/MAG. It could be also found in hybrid process. For instance, future work can be carried out to investigate these modes for MIG/MAG hybrid Laser, as shown in Figure 6.1.

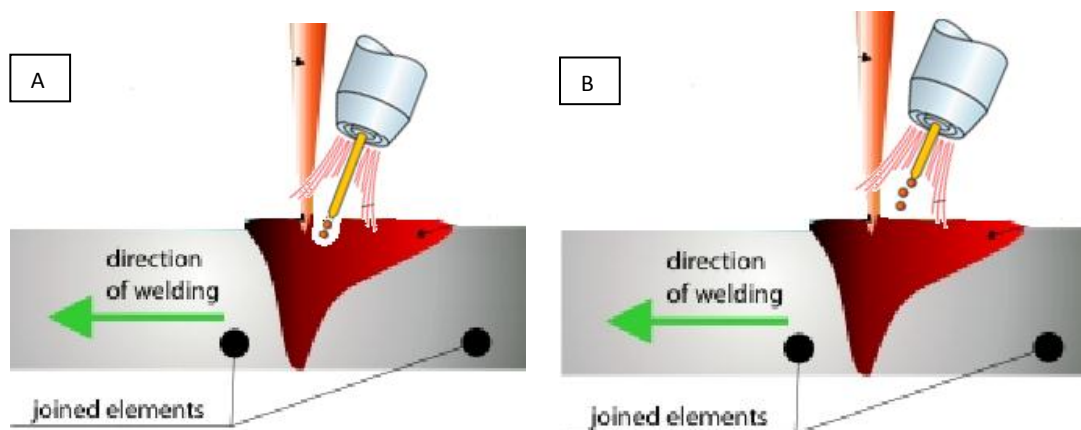


Figure 6.1: Schematic of metal transfer in MIG/MAG laser process. A) With buried B) Without buried

CHAPTER VII

References

- [1] AWS. Welding handbook, Chapter 5, **Flux cored arc welding**. Dan TN 2009.
- [2] CÍCERO. M. D.; PAULO. J. M.; ALEXANDRE. Q. B. Metal Transfer Study of a Rutilic Flux-Cored Wire. **Soldagem & Inspeção**, Ano 9, No. 4. Dezembro 2004.
- [3] LUZ, T. S.; RODRIGUES, C. E. A. L.; FERRARESI, V. A.; FARIAS, J. P.: Análise da Transferência Metálica do Arame Tubular em Comparação ao Arame Sólido. **CONEM, Belém**, PA. 2004.
- [4] MOTA, C.P., **Sistema de Visão por Infravermelho Próximo para Monitoramento de Processos de Soldagem a Arco**, in Pós-Graduação em Engenharia Mecânica, Universidade Federal de Uberlândia. 2011.
- [5] ASM. **Welding, Brazing and Soldering**, 1993.
- [6] TOM, M.; LISA, M.; FRANK, D.; GARR. E.; FRANK. K. **Innershield wire FCAW-S welding guide**. Lincoln electric.1995.
- [7] LARRY, J. **Welding Skills, Processes and Practices for Entry-Level Welders: Book 2**, 1st Edition, Lawrence Bower 2009.
- [8] LANCASTER, J. **The Physics of Welding**. New York: International Institute of Welding.1984.

- [9] IORDACHESCU, D.; QUINTINO, L.; Steps toward a New Classification of Metal Transfer in Gas Metal Arc Welding. **Journal of Materials Processing Technology**, 202, 391–397.2008.
- [10] LANCASTER, J. **The Physics of Welding**. 2 ed. Oxford: International Institute of Welding. 1986.
- [11] NORRISH, J. A Review of Metal Transfer Classification in Arc Welding (IIW DOC.XII-1769-03.Bucharest). Villepinte, France: **International Institute of Welding**.2003.
- [12] PONOMAREV, V.; SCOTTI, A.; SILVINSKIY, A.; AI-ERHAYEM, O. Atlas of MIG/MAG welding Metal Transfer Modes (IIW Doc. XII-1771 to 1775–03. Bucharest). Villepinte, France: **International Institute of Welding**.2003.
- [13] KAH et al.; Usability of Arc Types in Industrial Welding. **International Journal of Mechanical and Materials Engineering**. 2014.
- [14] WANG, G.; HUANG, PG.; ZHANG, YM. Numerical Analysis of Metal Transfer in Gas Metal Arc Welding Under Modified Pulsed Current Conditions. **Metallurgical and Materials Transactions B**, 35B, 857–866.2004.
- [15] NORRISH, J. **Advanced welding process**. IOP Publishing Ltd,. 375 p.ISBN:0-85274-325-4.1992.
- [16] ABDULLAH, B. M.; SMITH, J. S.; LUCAS, W.; LUCAS, J.; HOUGHTON, M. A Low Cost Vision System for Real-Time Monitoring of Welding Applications. **14th International Conference on the Joining of Materials & the 5th International Conference on Education in Welding**. Helsingor, Denmark. 29th of April - 2nd of May. 13 p.2007.
- [17] VILARINHO, L.O., et al., Sistema de Visão por infravermelho próximo Dedicado ao Monitoramento de Processo de Soldagem, in **VI Congresso Nacional de Engenharia Mecânica (CONEM)**. Gramado, RS, Brasil.2010.
- [18] BALSAMO PSS, et al. Development of an Experimental Technique for Studying Metal Transfer in Welding: Synchronized Shadowgraphy. **Int. J. for the Joining of Materials**. 2000.
- [19] HOUGHTON, M. A.; VILARINHO, L. O.; LUCAS, B.; LUCAS, J. J. Vision Systems for Monitoring and Control of Arc Welding Operations. **Soldagem e Inspeção**, v. 12, n. 4, p. 283-299, Out/Dez 2007.

- [20] OGAWA, Y. Observation of Weld Pool Behavior on TIG Welding. Proceedings of OMAE99, **18th International Conference On Offshore Mechanics and Arctic Engineering**. St. Johns, Newfoundland, Canada. July 11–16. 13 p.1999.
- [21] OGAWA, Y.; MORITA, T. Effect Of Shielding Gas And Wire Electrode On MIG Welding. Proceedings of OMAE99, **18th International Conference on Offshore Mechanics and Arctic Engineering**. St. Johns, Newfoundland, Canada. July 11–16. 13 p.1999.
- [22] CAROLINA, P. M.; MARCUS, V.; RIBEIRO, M.; ROBERTO, M. F. N.; LOURIEL O. V. Near-infrared Vision System for Monitoring Arc Welding Processes, **Welding International**, 29:3, 187-196, DOI: 10.1080/09507116.2014.932975.2015.
- [23] The company of Dataforth Europe. Industrial of data acquisition and control system, Available at: http://www.dataforth.com/dataacquisition.aspx?gclid=CIGRxO_ckMsCFUSAkQodNkMJvg Accessed in: May 2016.
- [24] FERNANDA, M, S. **A labview based synchronized data acquisition system with integrated webcam for welding processes**. Department of mechanical engineering. Federal university of Uberlandia, 2006.
- [25] LINCOLN. Flux-Cored Wire Selection. Available at: http://www.lincolnelectric.com/en-us/support/welding_solutions/Pages/shielded-flux-cored-electrodes.aspx . Accessed in: May 2016.
- [26] TOTALMATERIA. Filler Metals for Welding: Part One <http://www.keytometals.com/extended/page.aspx?ID=CheckArticle&site=kts&NM=71> . 2002, Accessed in: May 2016.
- [27] HEISERMAN, D. L. Shielded Metal-Arc Welding and Wearfacing. Available at: <http://free-ed.net/free-ed/Courses/05%20Building%20and%20Contruction/050205%20Welding/Welding00.asp?iNum=07> Accessed in: May 2016.
- [28] MOTA, C. P. **Sistema Guiado Sem Fio Para Soldagem Mecanizada Supervisionada Com Uso De Iluminação Por Infravermelho Próximo**. 2016. 223 f. Tese de Doutorado Universidade Federal de Uberlândia, Uberlândia.
- [29] FORTES, C. Arames Tubulares. **Apostila ESAB S/A**, Contagem, pp. 2-40.2004.
- [30] LINCOLN. Self-Shielded vs. Gas-Shielded Flux-Cored Electrodes. Available at: http://www.lincolnelectric.com/en-us/support/welding_solutions/Pages/shielded-flux-cored-electrodes.aspx . Accessed in: May 2016.

- [31] LI, K.; ZHANG, Y. Metal Transfer in Double-Electrode Gas Metal Arc Welding. **Manufacturing Science and Engineering**, 129(6), 991–999.2007.
- [32] WALL, W. A.; STEPHENS, D. L. Automatic Closed Circuit Television Electrode Guidance for Welding. **Welding Journal**, p. 713-720, 1969.
- [33] ISHIDE, T.; SHONO, S.; IIDA, Y.; FUJIWARA, M.; KAMO, K.; KONDO, Y. Development of Visual Sensor for Gas Shielding Arc Welding. **IIW Asian Pacific Regional Welding Congress and 36th Annual A.W.I. Conference**, Australian Welding Institute. 593-602 p.1988.
- [34] PITRUN, M. **The effect of welding parameters on levels of diffusible hydrogen in weld metal deposited using gas shielded rutile flux cored wires**, PhD thesis, Department of Materials engineering, university of Wollongong.2004.
- [35] SCOTTI, A.; PONOMAVEV, V. **Soldagem MIG/MAG: Melhor entendimento, melhor desempenho**. São Paulo, Artliber Editora, 284 p. 2008.